Aalborg Universitet

AALBORG UNIVERSITY
DENMARK

Distributed Power Sharing Control for Islanded Single-/Three-Phase Microgrids with Admissible Voltage and Energy Storage Constraints

Zhou, Jianguo; Sun, Hongbin; Xu, Yinliang; Han, Renke; Yi, Zhongkai; Wang, Liming; Guerrero, Josep M.

Published in:
IEEE Transactions on Smart Grid

DOI (link to publication from Publisher):
10.1109/TSG.2021.3057899

Publication date:
2021

Document Version
Accepted author manuscript, peer reviewed version

Link to publication from Aalborg University

Citation for published version (APA):
Zhou, J., Sun, H., Xu, Y., Han, R., Yi, Z., Wang, L., & Guerrero, J. M. (2021). Distributed Power Sharing Control for Islanded Single-/Three-Phase Microgrids with Admissible Voltage and Energy Storage Constraints. *IEEE Transactions on Smart Grid*, *12*(4), 2760-2775. Article 9351554. https://doi.org/10.1109/TSG.2021.3057899

General rights
Copyright and moral rights for the publications made accessible in the public portal are retained by the authors and/or other copyright owners and it is a condition of accessing publications that users recognise and abide by the legal requirements associated with these rights.

- Users may download and print one copy of any publication from the public portal for the purpose of private study or research.
- You may not further distribute the material or use it for any profit-making activity or commercial gain
- You may freely distribute the URL identifying the publication in the public portal -

Take down policy
If you believe that this document breaches copyright please contact us at vbn@aub.aau.dk providing details, and we will remove access to the work immediately and investigate your claim.

This article has been accepted for publication in a future issue of this journal, but has not been fully edited. Content may change prior to final publication. Citation information: DOI 10.1109/TSG.2021.3057899, IEEE Transactions on Smart Grid

Distributed Power Sharing Control for Islanded Single-/Three-Phase Microgrids with Admissible Voltage and Energy Storage Constraints

Jianguo Zhou, *Member, IEEE,* Hongbin Sun, *Fellow, IEEE,* Yinliang Xu, *Senior Member, IEEE,* Renke Han, *Member, IEEE,* Zhongkai Yi, Liming Wang, *Senior Member, IEEE,* and Josep M. Guerrero, *Fellow, IEEE*

***Abstract*—This paper investigates power sharing and power quality improvement issues of islanded single-/three-phase microgrids (S/T-MGs) where both sources and loads are unbalanced. A hierarchical distributed control approach is proposed, which consists of 1) a phase-independent virtual synchronous generator (P-VSG) control used for primary control of distributed generators (DGs), 2) a distributed secondary power flow regulator used for power sharing control among DGs and among phases, and 3) a distributed secondary voltage regulator used for voltage restoration and power quality improvement. Compared with conventional methods, the proposed control has several salient features: 1) the P-VSG control allows for independent and flexible power control and voltage regulation for each phase and accurate phase shifts; 2) distributed containment control proposed in the secondary power control and voltage regulation layer guarantees admissible output phase powers, voltage profiles and power quality; 3) the constraint operator developed for the secondary controllers makes charging/discharging power of the energy storage system (ESS) within permitted values; 4) communication delays are also considered in the proposed distributed approach. Simulation results are presented to demonstrate the proposed control method.**

***Index Terms*—single-/three-phase microgrids, power sharing, power quality, distributed control, phase-independent virtual synchronous generator.**

I. Introduction

MICROGRID (MG) has been regarded as a promising solution to integrate renewable energy sources (RESs) as well as distributed energy storage systems (ESSs), and has been widely studied including AC MGs [1], [3], DC MGs [2], and hybrid AC/DC MGs [4], being mainly focused on balanced MGs. However, the MG system is usually characterized by unbalance [5]–[7] due to the integration of single-phase distributed generators (SDGs)/loads and the occurrence of asymmetrical faults, leading to significant challenges for the secure and reliable operation of the MG. Such unbalanced systems could be found in different countries like Australia, Sweden and Germany [8], [9]. Take a real 415V low-voltage (LV) distribution system with 101 customers in Australia [8] as an example, 3 customers and 38 customers with photovoltaic (PV) generators are connected to the LV grid through three-phase and single-phase PV inverters, respectively.

Load power sharing and voltage regulation (including voltage quality enhancement) are the most important issues for microgrid operation, which is a challenging work in unbalanced S/T-MGs. Current research works in unbalanced MGs mainly include three aspects: i) power sharing control, ii) power quality control, and iii) simultaneous power sharing and power quality control. Approaches reported in literatures related to these research aspects can be divided into three categories: centralized, decentralized and distributed approaches.

For the first aspect, power sharing control in unbalanced MGs, various research works have been reported in literature [5], [10]–[15] and therein. These approaches are primarily based on droop control and virtual impedance control. For instance, He *et al.* [10] proposed a centralized approach to realize reactive power, imbalance power and harmonic power sharing based on virtual impedance regulation and droop control. Decentralized schemes have also been developed in literature [11], [12], where small-ac-signal injection method and single-phase droop control was proposed, respectively. To overcome the drawbacks of centralized and decentralized methods, authors in [5] proposed a distributed method to realize the above power sharing control objective. However, the above works mainly consider the unbalanced loads connected to the common bus. Unbalanced sources (Hybrid SDGs and three-phase DGs (TDGs)) are not considered while SDGs can be randomly integrated into the system besides TDGs in practice. Regarding this scenario, our previous work [13] proposed a power sharing unit (PSU) to manage the power flow between phases. The PSU is composed of three single-phase back-to-back (BTB) converters connected in a Δ-structure. Each BTB converter is connected between two phases. Thus, we can navigate the power flow between phases

Manuscript received March 25, 2020; revised August 1, 2020; revised October 26, 2020; accepted February 01, 2021. This work was supported in part by the National Natural Science Foundation of China under Grant (51907098, 51537006), in part by the China Postdoctoral Science Foundation under Grant 2020T130337 and in part by VILLUM FONDEN under the VILLUM Investigator Grant (no. 25920): Center for Research on Microgrids (CROM). Paper no. TSG-00432-2020. *(Corresponding author: Hongbin Sun and Yinliang Xu)*

J. Zhou, Y. Xu and Z. Yi are with the Tsinghua-Berkeley Shenzhen Institute (TBSI), Tsinghua Shenzhen International Graduate School (TsinghuaSIGS), Tsinghua University, 518055 Shenzhen, Guangdong, P. R. China. (e-mail: jg_zhou@sz.tsinghua.edu.cn; xu.yinliang@sz.tsinghua.edu.cn).

H. Sun is with the Department of Electrical Engineering, State Key Laboratory of Power Systems, Tsinghua University, 100084 Beijing, P. R. China. (e-mail: shb@tsinghua.edu.cn).

R. Han is with the Department of Engineering Science, University of Oxford, OX1 3PJ Oxford, U.K. (e-mail: renke.han@eng.ox.ac.uk).

L. Wang is with the Tsinghua Shenzhen International Graduate School (TsinghuaSIGS), Tsinghua University, 518055 Shenzhen, Guangdong, P. R. China. (email: wanglm@sz.tsinghua.edu.cn)

J. M. Guerrero is with the Center for Research on Microgrids (CROM), Department of Energy Technology, Aalborg University, 9220 Aalborg East, Denmark (Tel: +45 2037 8262; Fax: +45 9815 1411; e-mail: joz@et.aau.dk).

1949-3053 (c) 2021 IEEE. Personal use is permitted, but republication/redistribution requires IEEE permission. See http://www.ieee.org/publications_standards/publications/rights/index.html for more information.
Authorized licensed use limited to: Aalborg Universitetsbibliotek. Downloaded on February 15,2021 at 09:00:05 UTC from IEEE Xplore. Restrictions apply.

This article has been accepted for publication in a future issue of this journal, but has not been fully edited. Content may change prior to final publication. Citation information: DOI 10.1109/TSG.2021.3057899, IEEE Transactions on Smart Grid

to enhance the power supply reliability and RES utilization by controlling the PSU. A similar method was also proposed in [14], where BTB converters are also utilized between phases, and multi-segment droop method, intra- and inter-phase power control and management scenarios are considered in order to maintain desired voltage and frequency profiles. However, installing extra converters is required in [13] and [14], which could result in high costs. To address this issue, Karimi *et al.* [15] firstly developed decentralized modified $P-f$ droop functions to automatically perform the power flow among different phases through bidirectional four-leg TDGs in hybrid single-/three-phase microgrids (S/T-MG), where hybrid source PV/battery units were considered. However, better performance could be achieved via coordination between DGs instead of this decentralized method and how to determine the power of each phase is not discussed in detail. In unbalanced MGs, overloading of a phase could result in unnecessary DG tripping, load shedding, and reduce the overall system operation security and reliability. In [16], a dynamic power routing based optimal power flow method among phases was proposed to maximize the loadability of the hybrid AC/DC microgrids by using interlinking converters connected to the AC and DC subgrids, where all DGs' information is required for this centralized method. An event-based distributed method was proposed in [17] to balance the output power of TDGs. The basic idea of [16] and [17] is similar, but similar to [13], [14], both of them require extra equipments (ICs). Moreover, there is a lack of adequate coordination between TDGs and SDGs, and voltage quality also needs to be considered.

Although the above technologies can provide satisfactory power sharing performance, power quality control is another equally important issue in unbalanced MGs. The aim of the works discussed in [18]–[22] is predominantly to achieve unbalance voltage compensation among DGs. In [18], a customized power quality method using optimization was studied for different areas on the customer side. Similarly, a real-time supervisory control approach based on a scheduling framework was developed for voltage unbalance/harmonic improvement of multi-area MGs in [19]. Unlike these centralized methods, Li *et al.* [20] first proposed a standard data-driven controller for DGs via decentralized deep reinforcement learning with satisfactory power quality and Meng *et al.* [21] proposed a distributed method for voltage unbalance compensation. In [22], a three-phase electric spring was developed for voltage regulation and source current balancing in the unbalanced system. But, many electric springs shall be installed if used in a large-scale system. Moreover, only unbalanced loads are considered in the MGs in these works. Consequently, centralized approaches [23], [24] and master-slave method [25] were, respectively, developed to improve the voltage quality only using SDGs without coordination with TDGs. Also, it should be pointed out that power sharing control and power quality control should be simultaneously considered. The voltage magnitudes and voltage unbalance factors (VUF) should be regulated to fulfill the standard, e.g., IEEE 1547 standard [27] while designing power-sharing methods. Currently, only very few works explored this topic. For example, C. Burgos-Mellado *et al.* [28] proposed a cooperative control scheme based on the conservative power theory to share the unbalanced and distorted components of the currents and powers. And a secondary control loop was implemented to regulate the maximum voltage imbalance/distortion at the PCC. After that, a distributed version was developed in [29]. Nevertheless, these works still only discussed the unbalanced loads scenario.

Despite the significant research progress in the above aspects, there are still some obvious research gaps. i) Only are unbalanced loads considered in most of the existing works. Unbalanced sources with SDGs and TDGs are usually not considered except [13]–[16], where, however, they mainly focus on either power quality improvement or power sharing. Moreover, in [13], [14], [16], extra power converters or systems are required. ii) Coordination between SDGs and TDGs is not explored in most of the existing works like [15]. To the best of the authors' knowledge, only [26] considered this cooperation for unbalance compensation and balance operation of TDGs. More exploration is necessary for simultaneous power sharing and power quality improvement. iii) When considering unbalanced sources, conventional droop control [1] and VSG control [30] are not conductive to flexible regulation of power and voltage of each phase. Moreover, conventional secondary controllers, e.g., [2], [3], [5], [21], designed for accurate power sharing among DGs and voltage regulation could lead to TDG's phase of heavy load more easily overloaded and cannot guarantee voltage quality at all nodes fulling requirements.

With these motivations mentioned above, this paper focuses on power sharing and power quality issues of S/T-MGs. The main contributions can be summarized as follows:

1) Power sharing and power quality improvement of islanded S/T-MGs are investigated, where both DGs and loads are unbalanced, and hybrid RESs/ESSs are also considered. This is different from existing works, where only unbalanced loads and ideal dc sources are considered, or coordination between SDGs and TDGs is inadequately explored.

2) Different from conventional control approaches [1], [11], [30], [31], a phase-independent virtual synchronous generator (P-VSG) control is proposed for the primary control of DGs, which allows for independent and flexible power control and voltage regulation for each phase, and as well as accurately balanced phase shifts that make phase shifts balancing requirement and some negative effects avoided.

3) Distributed secondary containment controllers with communication delays are proposed for power sharing, voltage restoration and voltage quality control of SDGs/TDGs. Different from previous works like [2], [3], [5], [21], the proposed method with containment control and constraint operator can guarantee secure output phase powers, admissible voltage profiles, voltage quality, and charging/discharging power of ESSs, resulting in more secure and reliable operation.

The remainder of this paper is structured as follows. The notations, preliminaries and assumptions are briefly introduced in Section II. The S/T-MG system structure and problem formulation are presented in Section III. Section IV discusses the proposed control strategy and as well as the stability analysis. Simulation results are provided to validate our method in Section V. Conclusions are finally drawn in Section VI.

1949-3053 (c) 2021 IEEE. Personal use is permitted, but republication/redistribution requires IEEE permission. See http://www.ieee.org/publications_standards/publications/rights/index.html for more information.
Authorized licensed use limited to: Aalborg Universitetsbibliotek. Downloaded on February 15,2021 at 09:00:05 UTC from IEEE Xplore. Restrictions apply.

This article has been accepted for publication in a future issue of this journal, but has not been fully edited. Content may change prior to final publication. Citation information: DOI 10.1109/TSG.2021.3057899, IEEE Transactions on Smart Grid

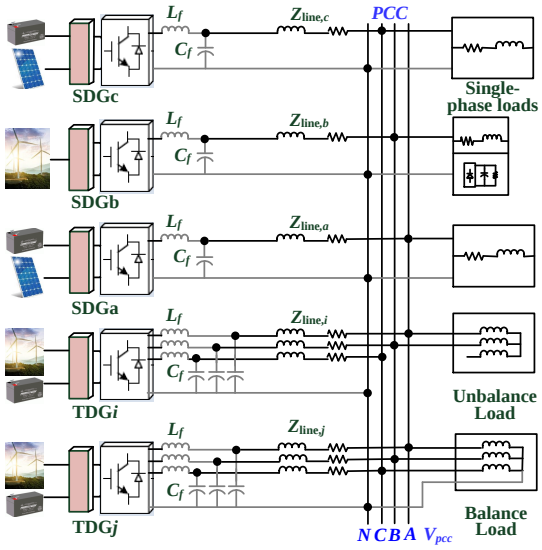

Fig. 1. A possible layout of a S/T-MG considered in this paper.

II. Notations, Preliminaries and Assumptions

Notations: $\mathcal{P}_{Y_{\mho}}(x)$ represents a projection of a vector x onto a closed convex set $Y_{\mho}$, i.e., $\mathcal{P}_{Y_{\mho}}(x) = \arg\min_{y\in Y}\|x-y\|$. Considering that x and y are one dimensional in this paper, the computation of the projection is then easily defined as

$$\mathcal{P}_{Y_{\mho}}(x) = \begin{cases} \mho^l_{\text{ref}}, & \text{if } x \le \mho^l_{\text{ref}} \\ x, & \text{if } \mho^l_{\text{ref}} < x < \mho^u_{\text{ref}} \\ \mho^u_{\text{ref}}, & \text{if } x \ge \mho^u_{\text{ref}} \end{cases}$$

where $\mho$ denotes the active power P, reactive power Q, voltage E and voltage unbalance factor VUF.

Graph Theory: Please refer to [2], [3] due to page limits.

Assumption 1: [32] Let $V_i \subseteq \Re^r, i = 1,\cdots,n$, be nonempty bounded closed sets such that for all i, $0 \in V_i$,

$$\max_{x\in V_i}\|S_{V_i}(x)\| = \overline{\rho}_i > 0, \quad \inf_{x\notin V_i}\|S_{V_i}(x)\| = \underline{\rho}_i > 0$$

where $\overline{\rho}_i$ and $\underline{\rho}_i$ are two positive constants, and $S_{V_i}(\cdot)$ is a constraint operator such that $S_{V_i}(0) = 0$ and when $x \neq 0$,

$$S_{V_i}(x) = \frac{x}{\|x\|}\max_{0\le\beta\le\|x\|}\left\{\beta|\frac{\alpha\beta x}{\|x\|}\in V_i, \forall 0\le\alpha\le 1\right\}.$$

Note that $\max_{x\in V_i}\|S_{V_i}(x)\| = \overline{\rho}_i > 0$ means that the state of charging (SoC) and charging/discharging power of all ESSs cannot be arbitrarily large and must be limited within the permitted values; and $\inf_{x\notin V_i}\|S_{V_i}(x)\| = \underline{\rho}_i > 0$ means that the SoC and charging/discharging power of all ESSs should not be less than the minimum values.

III. Structure of the S/T-MG and Problem Formulation

A. System Structure

Fig. 1 depicts a possible S/T-MG consisting of SDGs, TDGs, and single-phase and three-phase loads. The source of DGs can be PV, wind, hybrid PV/battery, or hybrid wind/battery. The SDGs are connected to the PCC through single-phase full bridge inverters with LC filters while three-phase four-wire inverters are adopted for TDGs. This type of MGs is typically an unbalanced system, which means that not only the load but also the DG units are unbalanced. Under this scenario, the output power of each phase of TDGs can be different from each other, which in turn affects the MG loadability and reliability. All the DG units in the MG should cooperate with each other to provide reliable power supply for the loads and guarantee proper load power sharing, admissible voltages, power quality and as well as ESS constraints. We will primarily focus on these issues in this work. And frequency regulation and as well as the zero sequence issue will not be discussed in the secondary control layer throughout the following paper. But it could be included if necessary.

B. Problem Formulation

As mentioned above, coordinated power sharing among different DGs including ESSs and among different phases of the TDGs in the S/T-MGs is very crucial and challenging due to the fast proliferation of different types of DG units and loads. The control objective of the S/T-MG includes the following three aspects:

1) Proper Power Sharing: The first objective of these DGs is to achieve proper real and reactive power sharing among them, which can be realized at the steady state if all units are ideally and properly controlled, i.e.,

$$\underbrace{k^{\text{TDG}}_{\text{p},1}P^{\text{TDG}}_1 = \cdots = k^{\text{TDG}}_{\text{p},N_{\text{TDG}}}P^{\text{TDG}}_{N_{\text{TDG}}}}_{\text{TDGs}} = \underbrace{k^{\text{SDG}}_{\text{p},1,\flat}P^{\text{SDG}}_{1,\flat} = \cdots = k^{\text{SDG}}_{\text{p},N_{\text{SDG\_}\flat},\flat}P^{\text{SDG}}_{N_{\text{SDG\_}\flat},\flat}}_{\text{SDGs, }\flat=a,b,c} \quad (1)$$

$$\underbrace{k^{\text{TDG}}_{\text{q},1}Q^{\text{TDG}}_1 = \cdots = k^{\text{TDG}}_{\text{q},N_{\text{TDG}}}Q^{\text{TDG}}_{N_{\text{TDG}}}}_{\text{TDGs}} = \underbrace{k^{\text{SDG}}_{\text{q},1,\flat}Q^{\text{SDG}}_{1,\flat} = \cdots = k^{\text{SDG}}_{\text{q},N_{\text{SDG\_}\flat},\flat}Q^{\text{SDG}}_{N_{\text{SDG\_}\flat},\flat}}_{\text{SDGs, }\flat=a,b,c} \quad (2)$$

where $k^{\text{TDG}}_{\text{p},i}$, $k^{\text{TDG}}_{\text{q},i}$, $k^{\text{SDG}}_{\text{p},j,\flat}$, and $k^{\text{SDG}}_{\text{q},j,\flat}$, $i = 1,\cdots,N_{\text{TDG}}$, $j = 1,\cdots,N_{\text{SDG\_}\flat}$ are the power sharing coefficients or droop slopes of droop control; $\flat = a,b,c$ represents phase-a, phase-b and phase-c.

For TDG i, $P^{\text{TDG}}_i = \sum_\flat P^{\text{TDG}}_{i,\flat}$, $Q^{\text{TDG}}_i = \sum_\flat Q^{\text{TDG}}_{i,\flat}$, under balanced operation condition, (3) and (4) should be satisfied

$$P^{\text{TDG}}_{i,a} = P^{\text{TDG}}_{i,b} = P^{\text{TDG}}_{i,c} \quad (3)$$

$$Q^{\text{TDG}}_{i,a} = Q^{\text{TDG}}_{i,b} = Q^{\text{TDG}}_{i,c}. \quad (4)$$

Therefore, from the above two aspects, the power balancing sharing objective under ideal conditions can be summarized as

$$3k^{\text{TDG}}_{\text{p},i}P^{\text{TDG}}_{i,\flat} = 3k^{\text{TDG}}_{\text{p},j}P^{\text{TDG}}_{j,\flat} = k^{\text{SDG}}_{\text{p},r,\flat}P^{\text{SDG}}_{r,\flat} \quad (5)$$

$$3k^{\text{TDG}}_{\text{q},i}Q^{\text{TDG}}_{i,\flat} = 3k^{\text{TDG}}_{\text{q},j}Q^{\text{TDG}}_{j,\flat} = k^{\text{SDG}}_{\text{q},r,\flat}Q^{\text{SDG}}_{r,\flat} \quad (6)$$

where $i \neq j = 1,\cdots,N_{\text{TDG}}$, $r = 1,\cdots,N_{\text{SDG\_}\flat}, \flat = a,b,c$.

However, in the real world, it may be difficult and unnecessary to accurately realize the above control goals especially for the S/T-MGs. In the S/T-MGs, the output power of the each phase of the TDG is most likely to be different from each other, which can deteriorate the operating reliability, security

1949-3053 (c) 2021 IEEE. Personal use is permitted, but republication/redistribution requires IEEE permission. See http://www.ieee.org/publications_standards/publications/rights/index.html for more information.
Authorized licensed use limited to: Aalborg Universitetsbibliotek. Downloaded on February 15,2021 at 09:00:05 UTC from IEEE Xplore. Restrictions apply.

This article has been accepted for publication in a future issue of this journal, but has not been fully edited. Content may change prior to final publication. Citation information: DOI 10.1109/TSG.2021.3057899, IEEE Transactions on Smart Grid

and power quality. Therefore, the balancing of output phase powers of TDG units should be considered besides achieving proper power sharing among DGs. The output phase power of each TDG unit and as well as that of SDG unit should be kept within the permitted maximum value,

$$\begin{aligned} 0 \le k^{\sharp}_{\mathrm{p},i,\flat} P^{\sharp}_{i,\flat} < k^{\sharp}_{\mathrm{p},i,\flat} P^{\sharp,\max}_{i,\flat} \\ 0 \le k^{\sharp}_{\mathrm{q},i,\flat} Q^{\sharp}_{i,\flat} < k^{\sharp}_{\mathrm{q},i,\flat} Q^{\sharp,\max}_{i,\flat} \end{aligned} \tag{7}$$

where the superscript $\sharp$ = TDG or SDG, $P^{\sharp,\max}_{i,\flat} = S^{\sharp}_{i,\flat}$, $Q^{\sharp,\max}_{i,\flat} = \sqrt{S^{\sharp}_{i,\flat} - P^{\sharp}_{i,\flat}}$, and $S^{\sharp}_{i,\flat}$ is the apparent power. For $\sharp$ = TDG, $k^{\mathrm{TDG}}_{\mathrm{p},i,\flat} = 3k^{\mathrm{TDG}}_{\mathrm{p},i}$ and $k^{\mathrm{TDG}}_{\mathrm{q},i,\flat} = 3k^{\mathrm{TDG}}_{\mathrm{q},i}$. For better readability and simplicity, "$\sharp$" is omitted throughout the following paper.

With this consideration, the accuracy of power sharing among DGs could be compromised. Therefore, the power sharing control performance, in this paper, is designed as

$$\lim_{k\to+\infty} \left\| x_{\mathrm{p},i,\flat}(k) - \mathcal{P}_{Y_P}\left(x_{\mathrm{p},i,\flat}(k)\right) \right\| = 0 \tag{8}$$

$$\lim_{k\to+\infty} \left\| x_{\mathrm{q},i,\flat}(k) - \mathcal{P}_{Y_Q}\left(x_{\mathrm{q},i,\flat}(k)\right) \right\| = 0 \tag{9}$$

where $x_{\mathrm{p},i,\flat}(k) = k_{\mathrm{p},i,\flat} P_{i,\flat}(k)$, $x_{\mathrm{q},i,\flat}(k) = k_{\mathrm{q},i,\flat} Q_{i,\flat}(k)$, $Y_P = \{[P^l_{\mathrm{ref}}, P^u_{\mathrm{ref}}]\}$, $Y_Q = \{[Q^l_{\mathrm{ref}}, Q^u_{\mathrm{ref}}]\}$, $P^l_{\mathrm{ref}} = 0$, $Q^l_{\mathrm{ref}} = 0$, $P^u_{\mathrm{ref}} = k_{\mathrm{p},i,\flat} P^{\max}_{i,\flat}$, $Q^u_{\mathrm{ref}} = k_{\mathrm{q},i,\flat} Q^{\max}_{i,\flat}$. This means that we make the power sharing among DG units asymptotically converge to the convex hull rather than mandate accurate power sharing among DG units, which could maintain the system operation reliability and security.

2) Admissible Voltage Profiles and Power Quality: Another important performance criterion in a S/T-MG is to maintain acceptable output voltage profiles. Firstly, node voltages need to be regulated to be close to the rated values, $E^* - \varepsilon^{\max} \le E_{i,\flat} \le E^* + \varepsilon^{\max}$ where E^* is the desired DG voltage magnitude and $\varepsilon^{\max}$ is the maximum permitted voltage regulation requirement (usually 3% of the rated voltage from the IEEE 1547 standard [27]). That is to say, voltages should converge to the convex hull spanned by voltage reference leaders

$$\lim_{k\to+\infty} \left\| E_{i,\flat}(k) - \mathcal{P}_{Y_{\mathrm{E}}}\left(E_{i,\flat}(k)\right) \right\| = 0 \tag{10}$$

where $Y_{\mathrm{E}} = \{[E^l_{\mathrm{ref}}, E^u_{\mathrm{ref}}]\}$, $E^l_{\mathrm{ref}} = E^* - \varepsilon^{\max}$, $E^u_{\mathrm{ref}} = E^* + \varepsilon^{\max}$.

Secondly, keeping acceptable voltage quality in the S/T-MG is also important, the VUF at each TDG node and PCC should not be larger than the allowed maximum value $\mathrm{VUF}^{\max}$ (usually 2% defined by IEEE 1547 standard [27]), i.e.,

$$\lim_{k\to+\infty} \left\| \mathrm{VUF}^{\mathrm{TDG}}_i(k) - \mathcal{P}_{Y_{\mathrm{VUF}}}\left(\mathrm{VUF}^{\mathrm{TDG}}_i(k)\right) \right\| = 0 \tag{11}$$

where $Y_{\mathrm{VUF}} = \{[\mathrm{VUF}^l_{\mathrm{ref}}, \mathrm{VUF}^u_{\mathrm{ref}}]\}$, $\mathrm{VUF}^l_{\mathrm{ref}} = 0$, $\mathrm{VUF}^u_{\mathrm{ref}} = \mathrm{VUF}^{\max}$, $\mathrm{VUF}^{\mathrm{TDG}}_i = 100\% \frac{E^{\mathrm{TDG},-}_i}{E^{\mathrm{TDG},+}_i}$, where $E^{\mathrm{TDG},-}_i = |e^{\mathrm{TDG},-}_i|$ and $E^{\mathrm{TDG},+}_i = |e^{\mathrm{TDG},+}_i|$ are respectively the voltage negative and positive sequence magnitude derived by symmetrical component analysis, i.e., $e^{\mathrm{TDG},+}_i = \frac{1}{3}(e^{\mathrm{TDG}}_{i,a} + \boldsymbol{a} e^{\mathrm{TDG}}_{i,b} + \boldsymbol{a}^2 e^{\mathrm{TDG}}_{i,c})$, $e^{\mathrm{TDG},-}_i = \frac{1}{3}(e^{\mathrm{TDG}}_{i,a} + \boldsymbol{a}^2 e^{\mathrm{TDG}}_{i,b} + \boldsymbol{a} e^{\mathrm{TDG}}_{i,c})$, $\boldsymbol{a} = 1\angle 120°$. $e^{\mathrm{TDG}}_{i,\flat}, \flat = a, b, c$ are the measured three-phase voltages.

3) Meeting ESS Constraints: ESSs are considered in our research work. The SoC and charging/discharging power of the ESSs should be maintained within permitted values for the sake of security and reliability, i.e.:

$$-P^{\mathrm{ch,max}}_{\mathrm{ess},i} < P_{\mathrm{ess},i} < P^{\mathrm{dch,max}}_{\mathrm{ess},i} \tag{12}$$

$$S^{\min}_{\mathrm{oC},i} < S_{\mathrm{oC},i} < S^{\max}_{\mathrm{oC},i} \tag{13}$$

where $S_{\mathrm{oC},i}$ and $P_{\mathrm{ess},i}$ are, respectively, the SoC and charging and discharging power of ESSs; $P^{\mathrm{ch,max}}_{\mathrm{ess},i}$ and $P^{\mathrm{dch,max}}_{\mathrm{ess},i}$ are, respectively, the permitted maximum charging and discharging power of ESSs; $S^{\min}_{\mathrm{oC},i}$ and $S^{\max}_{\mathrm{oC},i}$ are, respectively, the minimum and maximum SoC of ESSs. The discrete dynamic of the SoC can be described as [33]

$$S_{\mathrm{oC},i}(k+1) = (1-\gamma_i) S_{\mathrm{oC},i}(k) + \eta_{\mathrm{ess},i} C^{-1}_{\mathrm{ess},i} T P_{\mathrm{ess},i}(k) \tag{14}$$

where $\eta_{\mathrm{ess},i}$ and $C_{\mathrm{ess},i}$ are the charging/discharing efficiency and capacity of the ESSs, respectively; γ_i and T are self-discharging coefficient and time interval, respectively.

IV. Proposed Control Strategy for The S/T-MG

In this section, we present the proposed control strategy in detail, which includes 1) P-VSG controller and 2) secondary power sharing and voltage regulators. Then, we give the stability analysis and the proof.

A. P-VSG Control Used for Primary Control of DGs

In order to achieve flexible control and operation for the S/T-MG, we firstly propose a modified VSG control approach used for the primary control of DG units, which is given by

$$\dot{\theta}_{i,\flat} = \omega_{i,\flat} = \omega^* + \sum\nolimits_{\flat=a,b,c} \Delta\omega_{i,\flat} \tag{15}$$

$$M_i \Delta\dot{\omega}_{i,\flat} = P_{\mathrm{RES},i,\flat} + P_{\mathrm{ess},i,\flat} - P_{i,\flat} - D_{p,i} \Delta\omega_{i,\flat} \tag{16}$$

$$\begin{aligned} K_i \dot{E}_{i,\flat} = {} & Q_{\mathrm{set},i,\flat} + \Delta Q_{i,\flat} - Q_{i,\flat} \\ & - D_{q,i}\left(E_{i,\flat} - E^* - \Delta E_{i,\flat}\right) \end{aligned} \tag{17}$$

where ω^* is the desired angular frequency of the DG units, respectively; $\omega_{i,\flat}$ and $E_{i,\flat}$ are the output angular frequency and phase voltage magnitude of the DG units, respectively; $P_{i,\flat}$ and $Q_{i,\flat}$ are the output active and reactive powers of each phase, respectively; $P_{\mathrm{RES},i,\flat}$ and $P_{\mathrm{ess},i,\flat}$ are RES output power and ESS output power used for phase-$\flat$, respectively; $Q_{\mathrm{set},i,\flat}$ is reactive power set point of phase-$\flat$; $\Delta Q_{i,\flat}$ and $\Delta E_{i,\flat}$ are regulation terms of the reactive power and voltage magnitude of phase-$\flat$, respectively, which will be determined by the secondary controllers; M_i and $D_{p,i}$ are the virtual inertia and damping constants, respectively; K_i and $D_{q,i}$ are the integrator gain to regulate the field excitation and the voltage droop coefficient, respectively. Note that for SDG units, there is no sum of frequency deviations, and (15) can be rewritten as

$$\dot{\theta}_{i,\flat} = \omega^* + \Delta\omega_{i,\flat}. \tag{18}$$

Then, from (15)-(17), the reference voltage of TDG units, $\mathbf{e}^{\mathrm{TDG}}_i = (e^{\mathrm{TDG}}_{i,a}\ e^{\mathrm{TDG}}_{i,b}\ e^{\mathrm{TDG}}_{i,c})^\top$, can be generated by

$$\mathbf{e}^{\mathrm{TDG}}_i = \begin{pmatrix} E^{\mathrm{TDG}}_{i,a} \sin\left[\left(\omega^* + \sum \Delta\omega^{\mathrm{TDG}}_{i,\flat}\right) t\right] \\ E^{\mathrm{TDG}}_{i,b} \sin\left[\left(\omega^* + \sum \Delta\omega^{\mathrm{TDG}}_{i,\flat}\right) t - \frac{2\pi}{3}\right] \\ E^{\mathrm{TDG}}_{i,c} \sin\left[\left(\omega^* + \sum \Delta\omega^{\mathrm{TDG}}_{i,\flat}\right) t + \frac{2\pi}{3}\right] \end{pmatrix} \tag{19}$$

1949-3053 (c) 2021 IEEE. Personal use is permitted, but republication/redistribution requires IEEE permission. See http://www.ieee.org/publications_standards/publications/rights/index.html for more information.
Authorized licensed use limited to: Aalborg Universitetsbibliotek. Downloaded on February 15,2021 at 09:00:05 UTC from IEEE Xplore. Restrictions apply.

This article has been accepted for publication in a future issue of this journal, but has not been fully edited. Content may change prior to final publication. Citation information: DOI 10.1109/TSG.2021.3057899, IEEE Transactions on Smart Grid

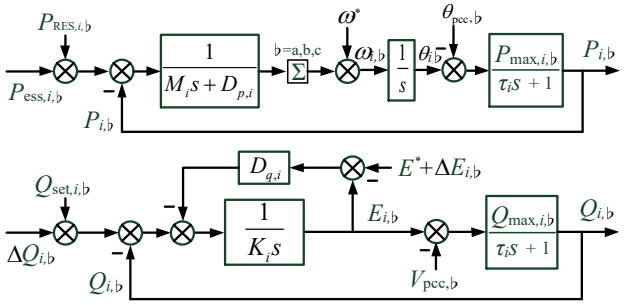

Fig. 2. The simplified control diagram of the P-VSG-controlled DGs.

where $\flat = a, b, c$. And the reference voltage of SDG units connected to phase-$\flat$ is given by

$$\mathbf{e}_{i,\flat}^{\text{SDG}} = E_{i,\flat}^{\text{SDG}} \sin\left[\left(\omega^* + \Delta\omega_{i,\flat}^{\text{SDG}}\right) t + \varphi_\flat\right] \tag{20}$$

where $\varphi_\flat$ is set as 0, $-\frac{2\pi}{3}$ and $\frac{2\pi}{3}$ for SDGs in phase-a, phase-b and phase-c, respectively. Note that $\varphi_\flat$ in (20) could be not a required term, but in order to keep a good voltage transient performance and make it easy to be understood, this term is remained here.

Remark 1: Compared with conventional VSG control like [30], [31], the proposed P-VSG control allows for independent and flexible power and voltage control for each phase. Specifically, i) for TDGs, the active and reactive power of each phase can be independently controlled by adjusting $P_{\text{ess},i,\flat}$ and $Q_{\text{set},i,\flat}$ to regulate $\Delta\omega_{i,\flat}$ and $E_{i,\flat}$, respectively, which facilitates the secondary controller design in the S/T-MG; ii) the voltage magnitude of each phase can also be independently controlled by regulating E^* thereby flexibly controlling the output voltage waveform if necessary for power quality control; iii) for TDGs, the sum of the frequency deviations among phases in (15), (19) and (21) can accurately guarantee balanced phase shifts of $\frac{2\pi}{3}$ thereby phase shifts balancing strategy and some negative effects can be avoided, which is also evaluated by the simulation results in Section V.

B. Distributed Secondary Control for Power Sharing and Voltage Regulation

The simplified control diagram of the proposed P-VSG controlled DG unit is shown in Fig. 2, where the dynamics of the LC filter, the RL output connector, and the voltage and current control loops are not considered since it is much faster than that of the P-VSG control loop. The active and reactive powers are usually processed through a low-pass filter and then fed to the control system. From Fig. 2, we have

$$\dot{P}_{i,\flat} = -\tau_i^{-1} P_{i,\flat} + \tau_i^{-1} P_{\max,i,\flat}\left(\theta_{i,\flat} - \theta_{\text{pcc},\flat}\right) \tag{21}$$

$$\dot{Q}_{i,\flat} = -\tau_i^{-1} Q_{i,\flat} + \tau_i^{-1} Q_{\max,i,\flat}\left(E_{i,\flat} - V_{\text{pcc},\flat}\right) \tag{22}$$

where τ_i is time constant of the low-pass filter; $P_{\max,i,\flat} = \frac{E^* V_{\text{pcc}}^*}{X_{\text{line},i}}$ and $Q_{\max,i,\flat} = \frac{E^*}{X_{\text{line},i}}$ are, respectively, the maximum active and reactive powers of each phase that can be delivered by the DG unit, and rated DG voltage and PCC voltage are adopted for simplicity. $X_{\text{line},i}$ is the coupling line parameter. Note that the model (21) and (22) is obtained based on the star-connected circuit but it is also applicable to the mesh-connected circuit via equivalent transformation operation.

Define variables

$$\dot{P}_{\text{ess},i,\flat} = u_{i,\flat}^P, \quad \Delta\dot{Q}_{i,\flat} = u_{i,\flat}^Q \tag{23}$$

$$\Delta\dot{E}_{i,\flat} = u_{i,\flat}^E, \quad \Delta\dot{E}_{i,\flat}^{\text{VUF}} = u_{i,\flat}^{\text{VUF}} \tag{24}$$

and $\overline{x}_i = \left(P_{i,\flat}, \theta_{i,\flat}, \Delta\omega_{i,\flat}, Q_{i,\flat}, E_{i,\flat}\right)^\top$, $x_i = \left(\overline{x}_i^\top, S_{\text{oC},i}\right)^\top$, $v_i = (P_{\text{ess},i,\flat}, \Delta Q_{i,\flat}, \Delta E_{i,\flat}, \Delta E_{i,\flat}^{\text{VUF}})^\top$,

$u_i = (u_{i,\flat}^P, u_{i,\flat}^Q, u_{i,\flat}^E, u_{i,\flat}^{\text{VUF}})^\top$,

$d_i = \left(\theta_{\text{pcc},\flat}, \sum_{\dagger,\dagger\neq\flat} \Delta\omega_{i,\dagger} + \omega^*, P_{\text{RES},i,\flat}, V_{\text{pcc}}, Q_{\text{set},i,\flat}, E^*\right)^\top$,

then, from (15)-(17) and (21)-(24), we have

$$\dot{\overline{x}}_i(t) = \overline{A}_i \overline{x}_i(t) + \overline{B}_i v_i(t) + \overline{D}_i d_i(t)$$
$$\dot{v}_i(t) = u_i(t)$$

In order to facilitate practical implementation of the proposed method, we discretize the above dynamic system

$$\overline{x}_i(k+1) = G_i \overline{x}_i(k) + H_i v_i(k) + F_i d_i(k)$$
$$v_i(k+1) = v_i(k) + T u_i(k)$$

where T is the sampling period. Then, combine this discrete-time dynamics and the dynamics (14), we can have the dynamics of the the DG unit in a compact discrete-time form

$$x_i(k+1) = A_i x_i(k) + B_i v_i(k) + D_i d_i(k) \tag{25}$$

$$v_i(k+1) = v_i(k) + T u_i(k) \tag{26}$$

$$y_i(k) = C_i x_i(k) \tag{27}$$

where $y_i(k)$ is the output variable; A_i, B_i, C_i and D_i are given in Appendix.

Therefore, the objective of this section is to design the secondary control schemes $u_i(k)$ such that the S/T-MG achieves the power sharing (8)-(9) and voltage regulation (10)-(11) goals while keeping ESSs' constraints (12)-(13) satisfied in a distributed framework. The overall schematic diagram of the proposed control policy for DG i is shown in Fig. 3, in which the controller consists of four separate modules: *primary P-VSG controller, active power balancing regulator*, *reactive power balancing regulator*, and *voltage regulator*.

1) Active Power Sharing Regulator: In order to balance the phase powers of TDGs while simultaneously maintaining proper power sharing among DG units and admissible SoC and charging/discharing power constraints, the phase active power $P_{i,\flat}^{\text{TDG}}$ of TDGs, the active power $P_{i,\flat}^{\text{SDG}}$ of SDGs and as well as $P_{\text{ess},i,\flat}$ are utilized to construct the controller

$$u_{i,\flat}^P(k) = S_{V_i}\left[P_{\text{ess},i,\flat}(k) - p_i P_{\text{ess},i,\flat}(k) + \pi_{i,\flat}(k)\right] \tag{28}$$

$$\pi_{i,\flat}(k) = \sum\nolimits_{j\in\mathcal{N}_i} a_{ij}\left[x_{\text{p},j,\flat}(k-\tau_{ij}) - x_{\text{p},i,\flat}(k)\right] - c\left[x_{\text{p},i,\flat}(k) - \mathcal{P}_{Y_P}\left(x_{\text{p},i,\flat}(k)\right)\right] \tag{29}$$

where $\tau_{ij} < \tau_{\max}$ is the communication time delay from agent j to agent i; p_i is the feedback damping gain of follower i; a_{ij} is the edge weight of the communication edge (j, i) and c is the pinning gain. If agent i can receive information directly from one or more leaders at time k, then $c > 0$ is

1949-3053 (c) 2021 IEEE. Personal use is permitted, but republication/redistribution requires IEEE permission. See http://www.ieee.org/publications_standards/publications/rights/index.html for more information.
Authorized licensed use limited to: Aalborg Universitetsbibliotek. Downloaded on February 15,2021 at 09:00:05 UTC from IEEE Xplore. Restrictions apply.

This article has been accepted for publication in a future issue of this journal, but has not been fully edited. Content may change prior to final publication. Citation information: DOI 10.1109/TSG.2021.3057899, IEEE Transactions on Smart Grid

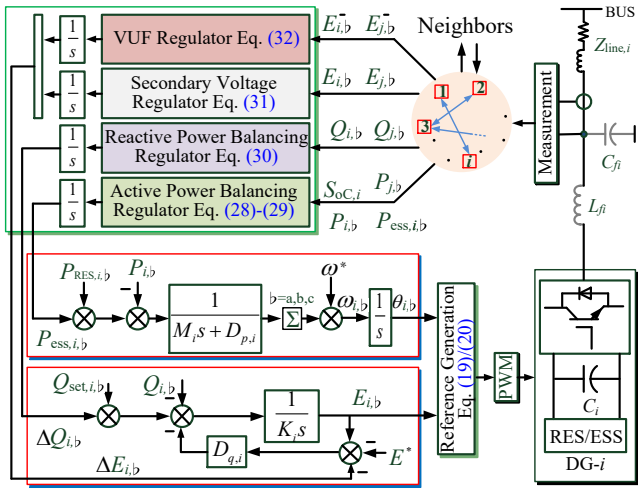

Fig. 3. Overall schematic diagram of the proposed control approach.

a positive constant; otherwise, $c = 0$. This guarantees proper active power sharing among DG units.

2) Reactive Power Sharing Regulator: The reactive power sharing strategy is similar to that of the active power sharing strategy. The phase reactive power $Q_{i,\flat}^{\text{TDG}}$ of TDGs, the reactive power $Q_{i,\flat}^{\text{SDG}}$ of SDGs are used to design the controller

$$u_{i,\flat}^{Q}(k) = \sum\nolimits_{j\in\mathcal{N}_i} a_{ij}\left[x_{\text{q},j,\flat}(k-\tau_{ij}) - x_{\text{q},i,\flat}(k)\right] - c\left[x_{\text{q},i,\flat}(k) - \mathcal{P}_{Y_Q}\left(x_{\text{q},i,\flat}(k)\right)\right]. \tag{30}$$

3) Voltage Regulator: The voltage regulator consists of two parts: a secondary voltage regulator and a voltage unbalance factor (VUF) regulator. In this part, the secondary voltage regulator is firstly designed to control the voltage of each DG unit close to rated voltage and within the admissible range (3% of the rated voltage from the IEEE 1547 standard [27]). Secondly, the VUF regulator is also designed for the TDGs to regulate the VUF to an acceptable value since admissible voltage range does not guarantee satisfied VUF. It could be more complicated if $\text{VUF}_i^{\text{TDG}}$ is directly used as the feedback information. So, we use the negative component of the voltage, $E_{i,\flat}^{\text{TDG},-}$, as the feedback signal in this work.

The secondary voltage regulator $u_{i,\flat}^{E}(k)$ and the VUF regulator $u_{i,\flat}^{\text{VUF}}(k)$ are, respectively, designed as

$$u_{i,\flat}^{E}(k) = \sum\nolimits_{j\in\mathcal{N}_i} a_{ij}\left[E_{j,\flat}(k-\tau_{ij}) - E_{i,\flat}(k)\right] - c\left[E_{i,\flat}(k) - \mathcal{P}_{Y_E}\left(E_{i,\flat}(k)\right)\right] \tag{31}$$

$$u_{i,\flat}^{\text{VUF}}(k) = \sum\nolimits_{j\in\mathcal{N}_i} a_{ij}\left[x_{j,\flat}^{\text{VUF}}(k-\tau_{ij}) - x_{i,\flat}^{\text{VUF}}(k)\right] - c\left[x_{i,\flat}^{\text{VUF}}(k) - \mathcal{P}_{Y_{\text{VUF}}}\left(x_{i,\flat}^{\text{VUF}}(k)\right)\right] \tag{32}$$

where $x_{i,\flat}^{\text{VUF}}(k) = E_{i,\flat}^{\text{TDG},-} = |e_{i,\flat}^{\text{TDG},-}|$ and $e_{i,a}^{\text{TDG},-} = e_i^{\text{TDG},-}$, $e_{i,b}^{\text{TDG},-} = \boldsymbol{a}e_{i,a}^{\text{TDG},-}$, $e_{i,c}^{\text{TDG},-} = \boldsymbol{a}^2 e_{i,a}^{\text{TDG},-}$.

Remark 2: Compared with existing literature, several differences of the proposed distributed control can be summarized as follows. *i*) For the secondary controller design, the system is formulated as an output containment control problem of multiple agents (25)-(27) with uncertain disturbances from RESs and constraints of ESSs. This is different from many existing literature where the disturbance and constraints are not considered. *ii*) Although accuracy of power sharing among DG units may be compromised, the distributed containment controllers (28)-(30) can guarantee that the output power of each phase is less than the maximum permitted value and that the unbalance of three-phase power of TDGs is improved, and controllers (31)-(32) make admissible voltage profiles and VUF satisfied, which is different from those of literature [2], [3], [5], [21]. *iii*) The constraint operator developed in the controller (28) makes charging/discharging power of the ESSs within permitted values, which is not considered in many studies where ideal sources are usually assumed. *iv*) Although the VUF regulator (32) is primarily designed for the TDGs in this work, it could be extended to be applicable to both TDGs and SDGs by assuming a virtual TDG for the SDG with virtual balanced three phase voltage that could be obtained by using a similar approach mentioned in Remark 3. Then, SDGs could coordinate with TDGs to regulate the VUF. *v*) Grid-following DGs usually regulate their output active and reactive power injected into the grid by measuring/estimating the angle and frequency of the bus voltage using a phase-locked loop (PLL) [40] and their power response from the reference power can be simply modeled as a first-order system [41]. Then the model similar to (25)-(27) can be obtained. It is possible to extend the proposed approach to the scenario that grid-forming DGs and grid-following DGs coexist but still require deeper analysis and even validation through simulation and experiment. We leave this issue in the future work considering the page limits.

Remark 3: The average (DC component) active and reactive power of each phase of TDGs and as well as that of SDGs, which are utilized in (28)-(30), can be calculated by

$$P_{i,\flat} = 0.5E_{i,\flat}I_{i,\flat}\cos(\psi) \tag{33}$$

$$Q_{i,\flat} = 0.5E_{i,\flat}I_{i,\flat}\sin(\psi) \tag{34}$$

where $E_{i,\flat}$ and $I_{i,\flat}$ are, respectively, the output phase voltage and current magnitudes of the DGs; ψ is the phase deviation between the voltage and current. These parameters can be obtained by using the Fourier analyser block in Matlab/Simulink toolbox or the All-Pass-Filter-Based PLL Systems proposed in [34]. Alternatively, the active and reactive power can also be calculated based on the $\alpha\beta$ transformation and second-order generalized integrator (SOGI) [35]

$$P_{i,\flat} = e_{i,\alpha}i_{i,\flat,\alpha} + e_{i,\beta}i_{i,\flat,\beta} \tag{35}$$

$$Q_{i,\flat} = e_{i,\beta}i_{i,\flat,\alpha} - e_{i,\alpha}i_{i,\flat,\beta} \tag{36}$$

where $e_{i,\alpha}$, $e_{i,\beta}$ and $i_{i,\flat,\alpha}$, $i_{i,\flat,\beta}$ are given by

$$\left(e_{i,\alpha}\ e_{i,\beta}\right)^{\top} = \mathcal{T}\left(\widehat{e}_{i,a}\ \widehat{e}_{i,b}\ \widehat{e}_{i,c}\right)^{\top} \tag{37}$$

$$\left(i_{i,\flat,\alpha}\ i_{i,\flat,\beta}\right)^{\top} = \mathcal{T}\left(\widehat{i}_{i,a}\ \widehat{i}_{i,b}\ \widehat{i}_{i,c}\right)^{\top} \tag{38}$$

where $\mathcal{T} = \frac{2}{3}[1\ \ -\frac{1}{2}\ \ -\frac{1}{2};\ 0\ \ \frac{\sqrt{3}}{2}\ \ -\frac{\sqrt{3}}{2}]$.

For TDGs, we set $\widehat{e}_{i,\flat}^{\text{TDG}} = e_{i,\flat}^{\text{TDG}}$, $\widehat{i}_{i,\flat}^{\text{TDG}} = i_{i,\flat}^{\text{TDG}}$, $\widehat{i}_{i,\nu}^{\text{TDG}} = 0$, $\flat = a,b,c$, $\nu \neq \flat$, where $e_{i,\flat}^{\text{TDG}}$ and $i_{i,\flat}^{\text{TDG}}$ are the measured phase voltage and current. For SDGs, we could regard

1949-3053 (c) 2021 IEEE. Personal use is permitted, but republication/redistribution requires IEEE permission. See http://www.ieee.org/publications_standards/publications/rights/index.html for more information.
Authorized licensed use limited to: Aalborg Universitetsbibliotek. Downloaded on February 15,2021 at 09:00:05 UTC from IEEE Xplore. Restrictions apply.

This article has been accepted for publication in a future issue of this journal, but has not been fully edited. Content may change prior to final publication. Citation information: DOI 10.1109/TSG.2021.3057899, IEEE Transactions on Smart Grid

$(\widehat{e}_{i,a}^{\mathrm{SDG}}\ \widehat{e}_{i,b}^{\mathrm{SDG}}\ \widehat{e}_{i,c}^{\mathrm{SDG}})^T$ and $(\widehat{i}_{i,a}^{\mathrm{SDG}}\ \widehat{i}_{i,b}^{\mathrm{SDG}}\ \widehat{i}_{i,c}^{\mathrm{SDG}})^T$ as virtual three-phase voltage and current. Specifically, for SDGs connected into phase-$\flat$, we set $\widehat{e}_{i,\flat}^{\mathrm{SDG}} = e_{i,\flat}^{\mathrm{SDG}}$, $\widehat{i}_{i,\flat}^{\mathrm{SDG}} = i_{i,\flat}^{\mathrm{SDG}}$, $\widehat{i}_{i,\nu}^{\mathrm{SDG}} = 0$, $\flat = a, b, c$, $\nu \neq \flat$, and the other two virtual phase voltages $\widehat{e}_{i,\nu}^{\mathrm{SDG}}$ $(\nu \neq \flat)$ could be constructed by shifting the phase of $\frac{2\pi}{3}$ based on the voltage $\widehat{e}_{i,\flat}^{\mathrm{SDG}} = e_{i,\flat}^{\mathrm{SDG}}$. Take SDGa (SDG units in phase-a) as an example, we can set $\widehat{e}_{i,a}^{\mathrm{SDG}} = e_{i,a}^{\mathrm{SDG}} = E_{i,a}^{\mathrm{SDG}} \sin(\omega t + \delta)$, $\widehat{i}_{i,a}^{\mathrm{SDG}} = i_{i,a}^{\mathrm{SDG}}$, $\widehat{i}_{i,b}^{\mathrm{SDG}} = \widehat{i}_{i,c}^{\mathrm{SDG}} = 0$, and then $\widehat{e}_{i,b}^{\mathrm{SDG}} = E_{i,a}^{\mathrm{SDG}} \sin(\omega t + \delta - \frac{2\pi}{3})$, $\widehat{e}_{i,c}^{\mathrm{SDG}} = E_{i,a}^{\mathrm{SDG}} \sin(\omega t + \delta + \frac{2\pi}{3})$. $\widehat{e}_{i,b}^{\mathrm{SDG}}$ and $\widehat{e}_{i,c}^{\mathrm{SDG}}$ are obtained with a phase shift of $\frac{2\pi}{3}$ based on the measured voltage $e_{i,a}^{\mathrm{SDG}} = E_{i,a}^{\mathrm{SDG}} \sin(\omega t + \delta)$, which can be realized by combining simple mathematical operations and SOGI [35]. Therefore, the active and reactive power can be obtained using (35)-(38). But the active and reactive power calculated by using the this approach has the oscillation component at the double fundamental frequency. The third method is based on the measured phase voltage and current of DGs, self-tuned notch filter and low pass filter. More details about this method can be found in [11]. In this paper, the first approach is adopted.

C. Stability Analysis

In order to analyze the convergence of the S/T-MG system, we first make the following model transformation.

Define $\beta_i = \frac{\left\| S_{V_i}\left[v_i(k) - p_i v_i(k) + \pi_{i,\flat}(k)\right] \right\|}{\left\| v_i(k) - p_i v_i(k) + \pi_{i,\flat}(k) \right\|}$ for all $k > 0$. Obviously, $0 < \beta_i \leq 1$. From the definition of the constraint operator $S_{V_i}(\cdot)$ and the controller $u_i(k)$ given by (28)-(32), we have

$$\begin{aligned} &S_{V_i}\left[v_i(k) - p_i v_i(k) + \pi_i(k)\right] \\ &\quad = \beta_i\left[v_i(k) - p_i v_i(k)\right] + \beta_i \pi_i(k) \end{aligned} \tag{39}$$

where $\pi_i(k) = -\sum_{j\in\mathcal{N}_i} a_{ij}\left[C_i x_i(k) - C_j x_j(k - \tau_{ij})\right] - c\left[C_i x_i(k) - \mathcal{P}_{Y_i}(C_i x_i(k))\right]$. We define $\phi_i(k) = \left[x_i^T(k), v_i^T(k)\right]^\top$, then, the DG system (25)-(26) with the corresponding controllers (28)-(32) can be written as the following closed-loop system form:

$$\begin{aligned} \phi_i(k+1) = &\mathbf{A}_i \phi_i(k) + \sum\nolimits_{j\in\mathcal{N}_i} a_{ij}\mathbf{A}_j \phi_j(k - \tau_{ij}) \\ &+ \mathbf{B}_i \mathcal{P}_{Y_i}\left(\mathbf{C}_i \phi_i(k)\right) + \mathbf{D}_i d_i(k) \end{aligned} \tag{40}$$

where the matrix parameters are given in Appendix. Then, we have the following Theorem.

Theorem 1: Assume that the communication graph $\mathcal{G}$ is connected and there exists at least one DG that can achieve the leader's reference information. Under Assumption 1, the DG agent system (25)-(27) of the S/T-MG can solve the containment active/reactive power sharing (8)-(9), voltage regulation (10) and power quality improvement (11) control problems by using the proposed distributed controllers (28)-(32) while keeping ESSs constraints (12)-(13) satisfied.

Proof: The proof is presented in Appendix.

D. Tuning of Controller Parameters

1) Tuning of P-VSG Parameters: In the primary P-VSG controller (15)-(17), the time constant of the frequency loop τ_f and the time constant of the field excitation loop τ_v are, respectively, given as $\tau_f = \frac{M_i}{D_{p,i}}$ and $\tau_v \approx \frac{K_i}{\omega^* D_{q,i}}$ [30]. Hence, the virtual inertia M_i and the gain K_i can be determined by $M_i = D_{p,i}\tau_f$ and $K_i = D_{q,i}\tau_v$, if we have decided the constant τ_f that can be chosen similar or much smaller compared to the case of a physical synchronous generator and the constant τ_v that is often chosen much larger than τ_f [36]. Initially, $D_{p,i}$ can be chosen such that a frequency drop of 0.5% causes the torque to increase by 100% from its nominal value, $D_{q,i}$ can be chosen such that a voltage drop of 5% causes the reactive power to increase by 100% [37]. However, these parameters may not be directly used or optimized values, and a specific method presented in [38] could be used to improve the parameter tuning.

2) Tuning of Secondary Controller Parameters: For the secondary controllers, two parameters, i.e., p_i and c, need to be determined. According to the literature [32], the controller parameter p_i could be chosen to satisfy $0 < b_i(k) \leq p_i(k+1) < \frac{1}{T}$ for all $k \geq 0$, where $b_i(k)$ is defined as $b_i(k) = \frac{1 - \beta_i(k)(1 - p_i(k)T)}{T}$. With regard to the pinning gain c, it is set as $c = 1$ for all the agents when they can receive the information directly from the leaders.

V. Simulation Results

To validate the performance of the proposed control scheme for the S/T-MG under various conditions, the S/T-MG depicted in Fig. 1 is simulated in MATLAB/Simulink environment. The solver used is ode23tb with a relative tolerance of 10^{-3}, and the system sampling time is 0.1 ms. In Fig. 1, two TDGs, three SDGs connected to phase-A, phase-B and phase-C, and unbalanced loads are considered. A three H-bridge converter based three-phase four-wire DC-AC inverter with LC filters is adopted to interface the TDGs while a single-phase H-bridge inverter is used for the SDGs. The ratios of power ratings of DG units are considered as T-DG1:TDG2:SDGa:SDGb:SDGc=2:2:1:1:1. Parameters of the test microgrid system and the controllers are listed in Table I. The time constants of frequency and voltage loops are chosen to be $\tau_f = 0.002$ s and $\tau_v = 0.02$ s. For simplicity, the secondary controller parameter p_i is taken as $p_i = 10$ for all the agents. The agents' communication topology is shown in Fig. 4 in detail, in which each phase of the DG units including TDGs and SDGs has a dedicated control agent. These agents of the TDGs and SDGs that have the same phases are connected together forming a ring-shape communication topology for data exchange. In order to further validate the proposal, a five-busbar S/T-MG depicted in Fig. 5 is simulated in the last case, where balanced loads (L1 and L2) are connected at the bus of B1 and B2, respectively. And the loads La and Lc are, respectively, connected at Ba and Bc. There is no load connected at Bb.

A. Case 1: Performance Under Load Change and PnP

This case aims at validating the performance of proposed control approach under load change and plug-and-play (PnP) by comparing with the conventional method presented in [3] and [30]. At the beginning, the system is experiencing a balanced active and reactive power load demand. But the supply

1949-3053 (c) 2021 IEEE. Personal use is permitted, but republication/redistribution requires IEEE permission. See http://www.ieee.org/publications_standards/publications/rights/index.html for more information.
Authorized licensed use limited to: Aalborg Universitetsbibliotek. Downloaded on February 15,2021 at 09:00:05 UTC from IEEE Xplore. Restrictions apply.

This article has been accepted for publication in a future issue of this journal, but has not been fully edited. Content may change prior to final publication. Citation information: DOI 10.1109/TSG.2021.3057899, IEEE Transactions on Smart Grid

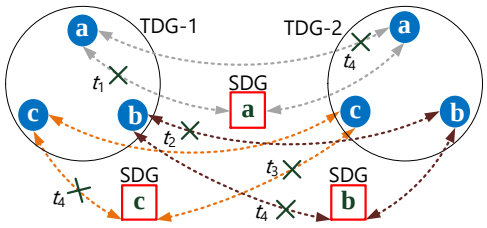

Fig. 4. Agents communication topology for the S/T-MG (TDG agents and SDG agents are represented by highlighted circle nodes and square nodes, respectively. "×" represents different link failures at different time t_i.)

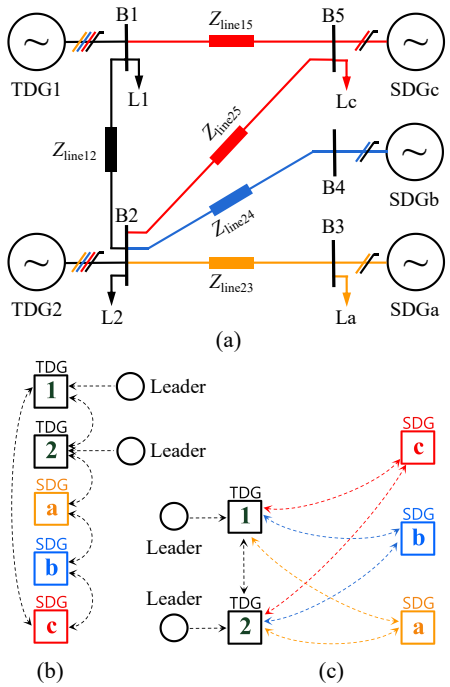

Fig. 5. Simulation test system for case 4. (a) Microgrid structure. (b) Communication topology for conventional approach. (c) Communication topology for the proposed approach.

is unbalanced, i.e., TDG1, TDG2 and SDGa provide power for the load together. And then, at $t = 1.5s$, the loads connected to phase-A and phase-B are increased. Consequently, the loads are also unbalanced. Finally, at $t = 5.5s$ and $t = 9s$, the DG units, SDGb and SDGc are, respectively, plugged into the microgrid, providing power supply for the system load demand together with TDG1, TDG2 and SDGa. The details are as follows.

1) Accurate Power Sharing Among DG Units (Conventional Approach): Fig. 6(a), Fig. 7(a) and Fig. 8(a) show the performance of the conventional VSG control method in [30] and the distributed method in [3], where the steady state values of active and reactive powers are shown in Fig. 10. From $t = 3$ s, the conventional distributed method [3] designed for accurate power sharing among DGs (SDGs and TDGs) is activated. From the results, it can be obviously observed that proportional power sharing cannot be realized only using conventional VSG method due to line impedance, and that although the active and reactive power is proportionally shared among these DGs (The power sharing ratio is about 2.0:1.0:1.0:1.0

TABLE I
PARAMETERS OF THE SIMULATION TEST MICROGRID SYSTEM AND PROPOSED CONTROLLERS

Parameters	Symbol	Value	Unit
Nominal voltage	E^*	311	V
Nominal frequency	ω^*	$2\pi \times 50$	rad
DC voltage	-	650†	V
	-	400‡	V
DC capacitor	C_{dc}	2200	μF
Filter inductance	L_f	3	mH
Filter capacitor	C_f	15	μF
Power rating	$P_{i,\flat}^{\text{TDG,max}}$	5	kW
	$P_a^{\text{SDG,max}}$	7.5	kW
	$P_b^{\text{SDG,max}}$	7.5	kW
	$P_c^{\text{SDG,max}}$	7.5	kW
Line impedance	$Z_{line,i}$	0.2+j1.1	Ω
	$Z_{line,a}$	0.08+j1.8	Ω
	$Z_{line,b}$	0.1+j1.2	Ω
	$Z_{line,c}$	0.1+j0.8	Ω
Virtual inertia	M_i	0.04	kW·s^2
Virtual damping	$D_{p,i}$	19.7	kW/Hz
Virtual gain	K_i	7.5	-
Droop coefficient	$D_{q,i}$	6†	kVar/V
		3‡	kVar/V
Sampling time	T	0.1	ms
Feedback damping gains	p_i	10	-
Pinning gains	c	1	-

† TDGs; ‡ SDGs.

(TDG1:TDG2:SDGa:SDGb:SDGc).), the admissible voltage profile cannot be guaranteed, some voltages (SDGa, SDGb and SDGc) are beyond the boundary (300V-320V, 3% of rated voltage) during the time of $t = 3 - 5.5s$, $t = 5.5 - 9s$ and $t = 9 - 12s$, respectively. More over, the discharging powers of SDGb and SDGc ($P_{\text{ess},b}^{\text{SDG}} = 2.912$ kW, $P_{\text{ess},c}^{\text{SDG}} = 2.596$ kW) are larger than maximum permitted value 2.5 kW, which could be harmful to the operation of ESS system. Additionally, the VUF at the PCC is higher than 2% during $t = 3 - 5.5s$ and $t = 9 - 12s$, which may not be acceptable according to the IEEE 1547 standard [27]. The results shown in Fig. 8(a) demonstrate that PnP, stable frequency response, an accurate phase shift of 120° of the output voltage can be achieved with conventional method. The maximum phase difference (The definition of the index, phase difference, is the same as that proposed in [11].) at steady state is about 0.36°.

2) Control Performance with Proposed Approach: The proposed control approach is activated in this test where load condition is the same as that of the above test, and the results are presented in Fig. 6(b), Fig. 7(b) and Fig. 8(b), where the steady state values of active and reactive powers are shown in Fig. 10. Before the time of $t = 3$ s, only the proposed P-VSG method is implemented. It can be observed that the control performance of the proposed method is comparable to that of the traditional method, which validates the effectiveness of the P-VSG. After $t = 3$ s, the proposed distributed containment controllers (28), (29), (30), (31) and (32) are activated for active and reactive power sharing, voltage

1949-3053 (c) 2021 IEEE. Personal use is permitted, but republication/redistribution requires IEEE permission. See http://www.ieee.org/publications_standards/publications/rights/index.html for more information.
Authorized licensed use limited to: Aalborg Universitetsbibliotek. Downloaded on February 15,2021 at 09:00:05 UTC from IEEE Xplore. Restrictions apply.

This article has been accepted for publication in a future issue of this journal, but has not been fully edited. Content may change prior to final publication. Citation information: DOI 10.1109/TSG.2021.3057899, IEEE Transactions on Smart Grid

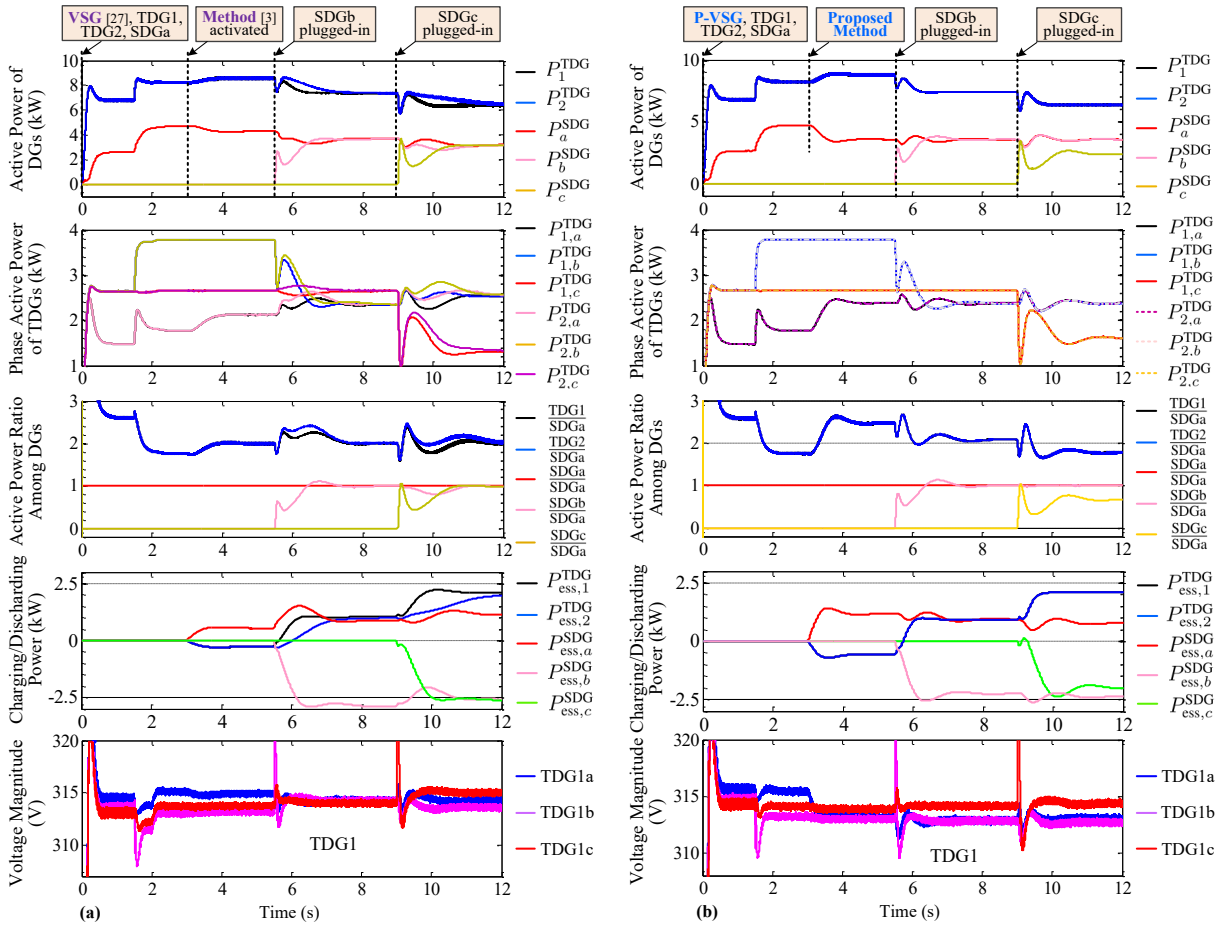

Fig. 6. Simulation results under case 1. (a) Conventional method. (b) Proposed method.

regulation and VUF control, respectively. Compared to the conventional method, some significant improvements can be easily observed once the proposed method is implemented. i) Although the accuracy of power sharing among DGs is compromised, the balancing performance of the TDGs' output three-phase power is improved, which can also be observed from Fig. 6(b), Fig. 7(b), Fig. 9 and Fig. 10. ii) Moreover, the output powers of each phase of TDGs and SDGs are more stable and resilient, which means that load change of one phase has little effect on the output powers of other phases (see Fig. 9) since DGs are inclined to share the load power according to the power ratings of each phase but not the ratings of DGs. iii) The voltages and the corresponding VUFs ($<$2%) are all regulated to fulfill the admissible requirements of the standard. The neutral current of TDGs is also reduced compared to that with conventional method (see Fig.8). iv) The charging/discharding power of the ESSs ($P^{\text{SDG}}_{\text{ess},b} = 2.25$ kW, $P^{\text{SDG}}_{\text{ess},c} = 2.02$ kW) is controlled to less than the maximum permitted value (2.5 kW) with the help of constraint operator. v) Seen from Fig. 8(b), an accurate phase shift of 120° of the output voltage of the three-phase converters is approximately achieved with the proposed P-VSG method. The maximum phase difference at steady state is about 0.35°. This validates the effectiveness of the proposed approach and as well as PnP capability. Note that some differences about the behaviour of phase shift could be observed compared to those obtained by using the conventional method, which is mainly caused by the differences from the primary and secondary controllers. The proposed secondary controllers along with the primary P-VSG controller will make $\sum \Delta\omega_b^{\text{TDG}}$ different from that obtained from the conventional method, which means that rate of change of phase shift is different and so is the behavior of phase shift.

B. Case 2: Communication Time-Delay and Link Failure

In this case, the effects of the communication time-delays are considered due to its ubiquitous existence in practical engineering applications and possible deterioration and instability of the system operation. The time-delay is set to be 20 ms, 40 ms, and 200 ms, respectively. Fig. 11 (a), (b) and (c) show the responses of DGs within the S/T-MG when the proposed controllers are applied at t = 2 s. It can be seen that the TDGs and SDGs can properly share the load power (see Fig. 11(a) and (b)) for the case of τ = 20 ms and τ = 40 ms. The system can converge to the steady state. But the longer the time delay, the worse the control performance. The control performance of output power and voltages of SDGs is much more seriously deteriorated. For the case of τ = 200 ms, neither the admissible voltages nor the admissible VUF can be achieved (Fig. 11(c)). The convergence rate is very slow. It will take much longer

1949-3053 (c) 2021 IEEE. Personal use is permitted, but republication/redistribution requires IEEE permission. See http://www.ieee.org/publications_standards/publications/rights/index.html for more information.
Authorized licensed use limited to: Aalborg Universitetsbibliotek. Downloaded on February 15,2021 at 09:00:05 UTC from IEEE Xplore. Restrictions apply.

This article has been accepted for publication in a future issue of this journal, but has not been fully edited. Content may change prior to final publication. Citation information: DOI 10.1109/TSG.2021.3057899, IEEE Transactions on Smart Grid

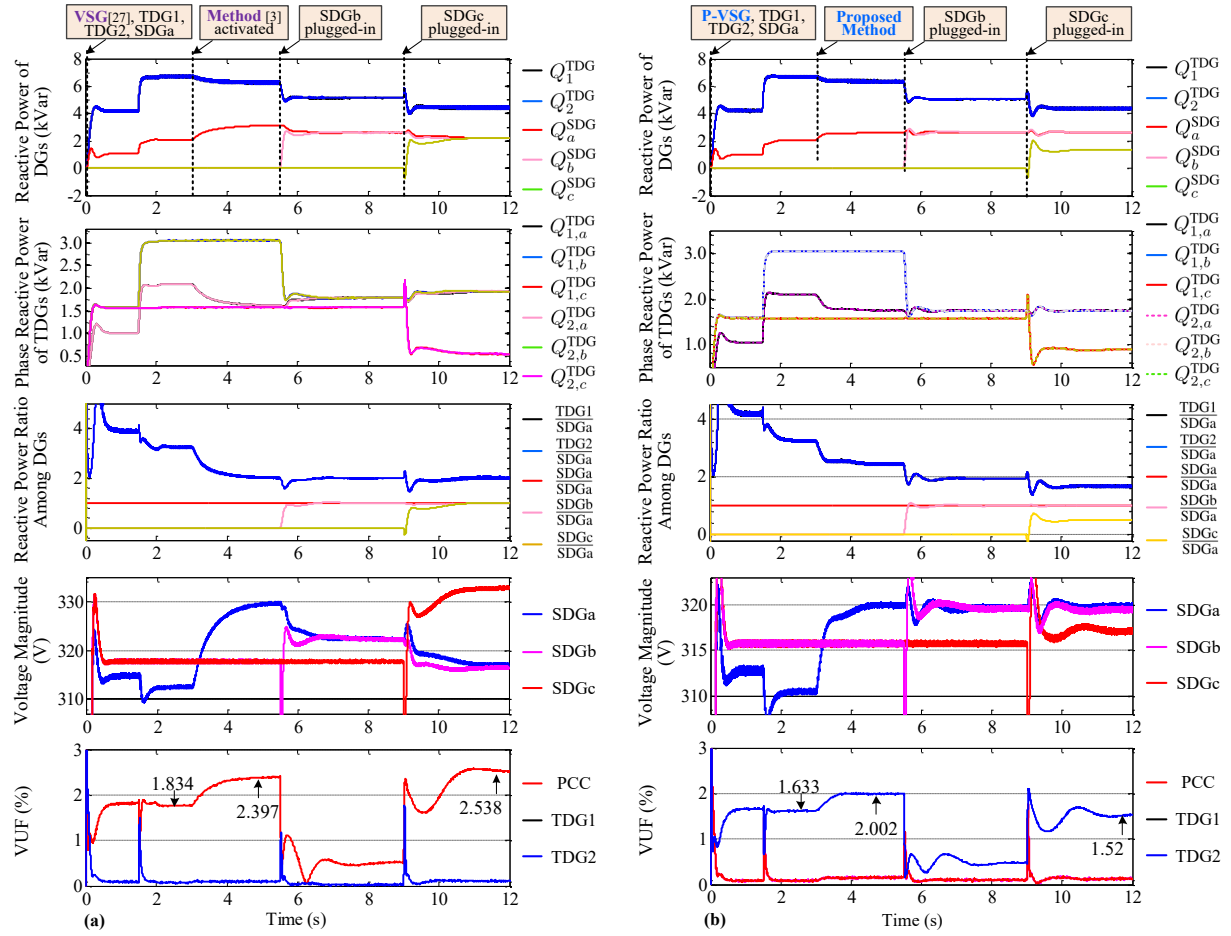

Fig. 7. Simulation results under case 1. (a) Conventional method. (b) Proposed method.

time for the system to converge to the steady state. But it still can be stabilized, which could satisfy the requirement of 100 ms time delay as an admissible value for control information in microgrids according to the IEC 61850 standard [39].

The scenario of communication link failures is studied in this case. A ring-shape topology is adopted for the communication of agents shown in Fig. 4, where the link failures are set as t_1 = 3 s, t_2 = 3.5 s, t_3 = 5 s, and t_4 = 6.5 s. Finally, at t = 8 s, the failed links are retrieved. Additional single-phase load is connected to phase-a and phase-c at t = 3.5 s and t = 5.5 s, respectively, and disconnected at t = 7 s. From the results shown in Fig. 12, the connectivity of the communication is maintained before t_4 = 6.5 s, so DGs can still share the load power as expected. Although connectivity in the graph is lost during 6.5 s $-$ 8 s, the output powers of DGs are maintained unchanged until the load is changed at t = 7 s due to the application of integrator. When the connectivity of the communication graph is established again after t = 8 s, the system can be brought back to the normal operation sate.

C. Case 3: The Scenario of All SDGs Connected to Phase-a

In this case, we consider a special scenario that all the SDGs are connected to phase-a. Two TDGs and two SDGs connected to phase-a are considered in the microgrid (see Fig. 5). During the time $t = 1 \sim 3.5$ s, conventional distributed

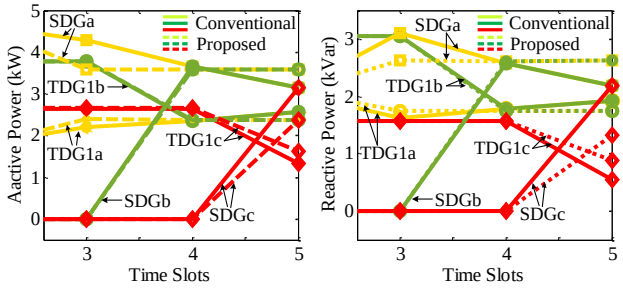

Fig. 9. Output powers of TDGs and SDGs at the steady state under case 1.

method is utilized for active power sharing while during the time $t = 3.5$ s to $t = 8$ s, the proposed distributed method for active power sharing is utilized. Finally, after $t = 8$ s, the conventional method is used again. At time $t = 6$ s, the generation unit, TDG1, is plugged out. From the results shown in Fig. 13, it can be observed that during the time $t = 3.5 \sim 6$ s, the unbalance is obviously improved by using the proposed approach compared to the response before the time $t = 3.5$ s by using the conventional approach. Moreover, the proposed approach doesn't result in reverse power flow on phase-a of TDG2 when TDG1 is plugged out at $t = 6$ s. However, the conventional method results in reverse power flow on this phase, which may cause adverse effects on the system. This

1949-3053 (c) 2021 IEEE. Personal use is permitted, but republication/redistribution requires IEEE permission. See http://www.ieee.org/publications_standards/publications/rights/index.html for more information.
Authorized licensed use limited to: Aalborg Universitetsbibliotek. Downloaded on February 15,2021 at 09:00:05 UTC from IEEE Xplore. Restrictions apply.

This article has been accepted for publication in a future issue of this journal, but has not been fully edited. Content may change prior to final publication. Citation information: DOI 10.1109/TSG.2021.3057899, IEEE Transactions on Smart Grid

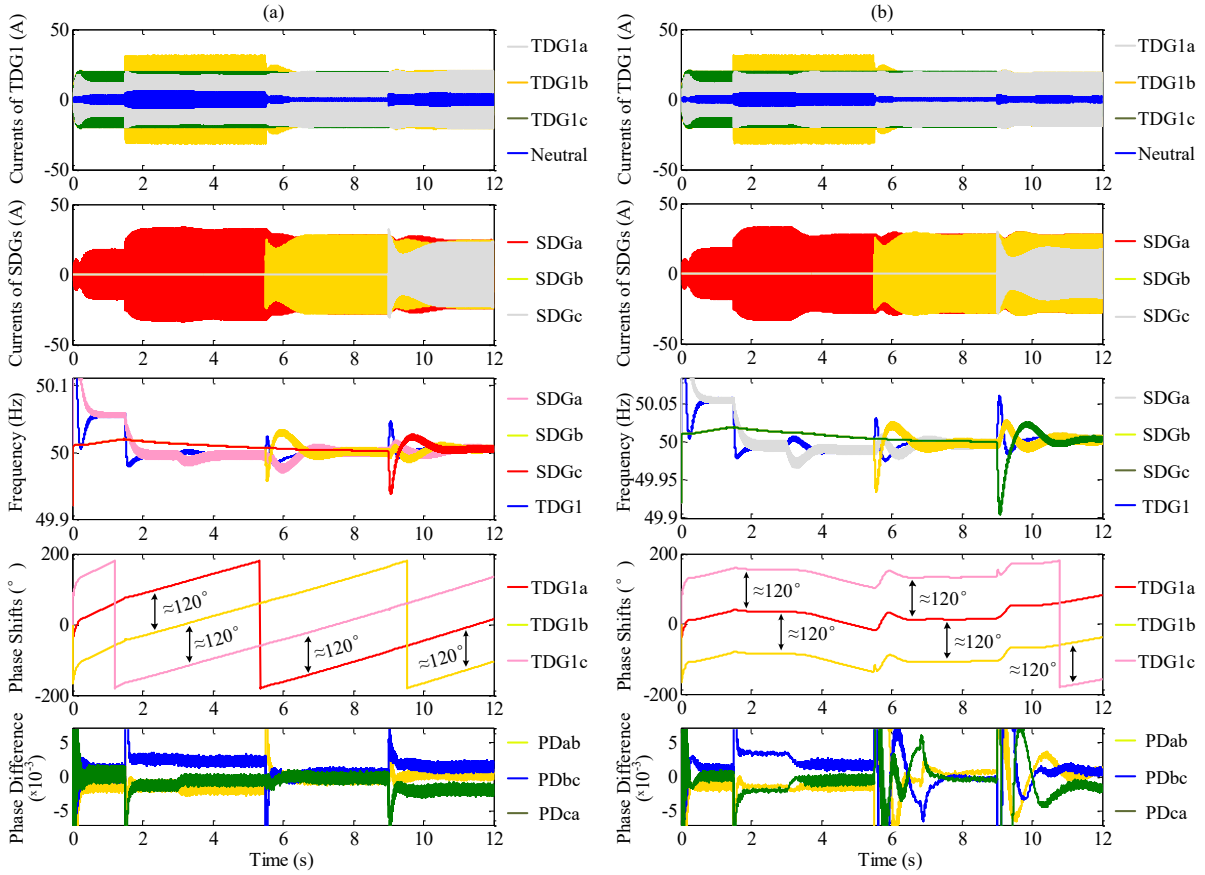

Fig. 8. Simulation results under case 1. (a) Results with conventional method. (b) Results with proposed method.

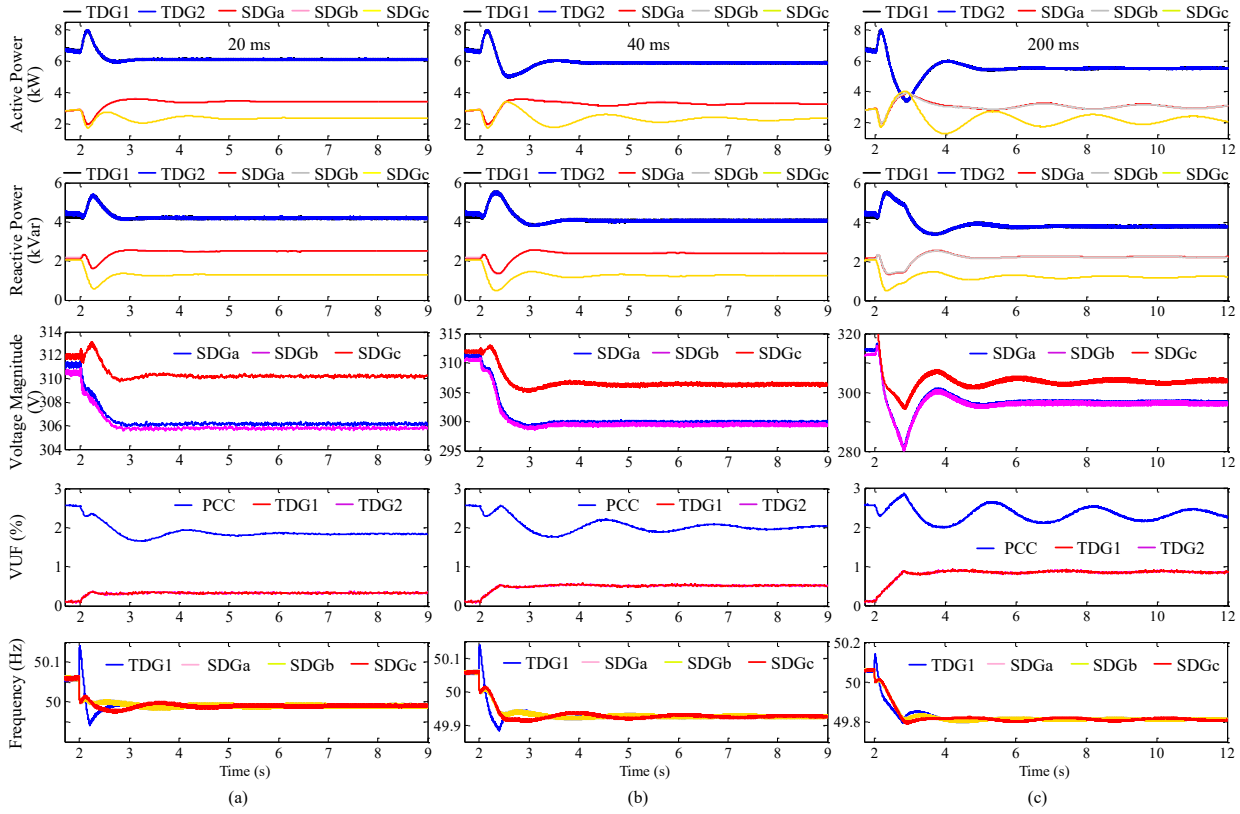

Fig. 11. System performance under different time-delays in case 2. (a) 20 ms time-delay. (b) 40 ms time-delay. (c) 200 ms time-delay.

1949-3053 (c) 2021 IEEE. Personal use is permitted, but republication/redistribution requires IEEE permission. See http://www.ieee.org/publications_standards/publications/rights/index.html for more information.
Authorized licensed use limited to: Aalborg Universitetsbibliotek. Downloaded on February 15,2021 at 09:00:05 UTC from IEEE Xplore. Restrictions apply.

This article has been accepted for publication in a future issue of this journal, but has not been fully edited. Content may change prior to final publication. Citation information: DOI 10.1109/TSG.2021.3057899, IEEE Transactions on Smart Grid

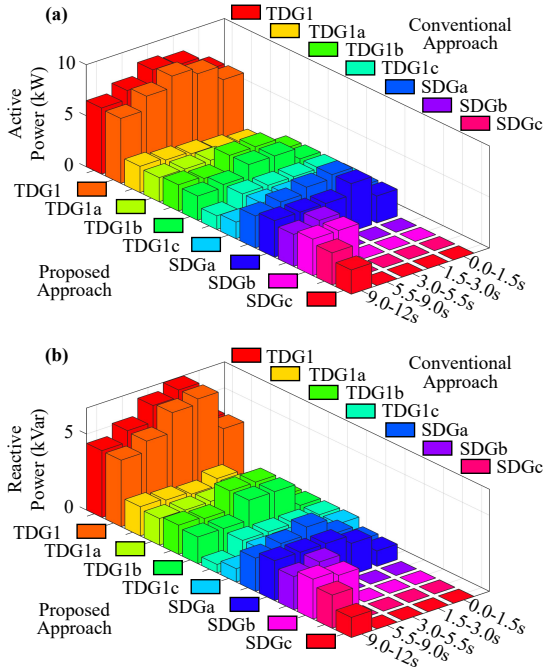

Fig. 10. Steady state values of active and reactive power of the simulation results shown in Fig. 6 and Fig. 7 under Case 1.

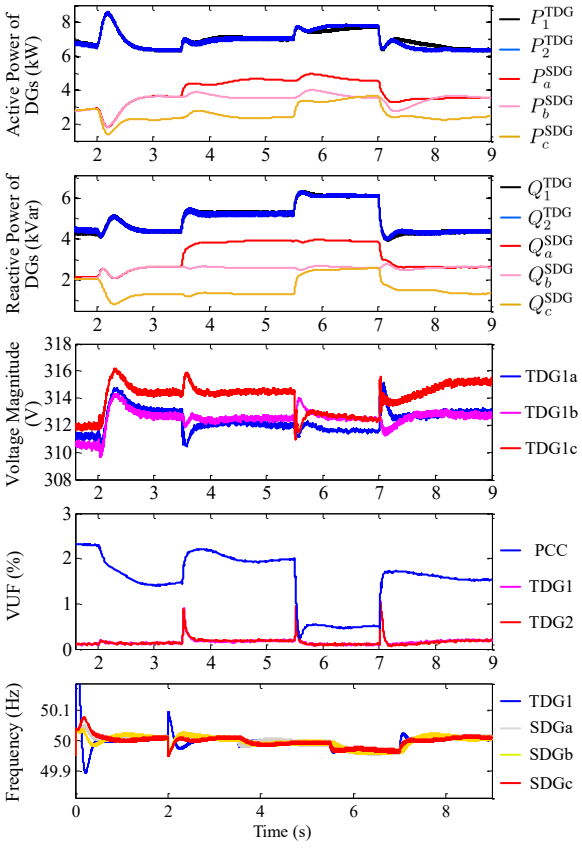

Fig. 12. System responses under link failures and load changes in case 2.

could be interpreted as that generation units on each phase share the load power based on their phase ratings instead of their total ratings. Using this way, phase-a of the three phase inverters and all the single phase inverters connected to this

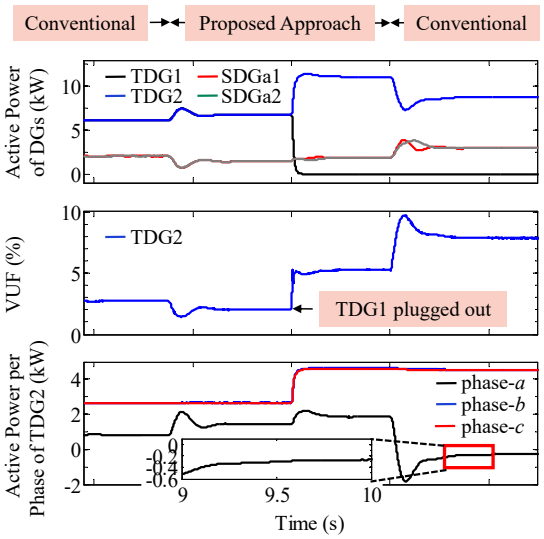

Fig. 13. System performance under case 3.

phase will share the load power on this phase based on their phase ratings. Therefore, it will create a positive output power of phase-a of the three phase inverter but not reverse power flow on it. This is different from the conventional method.

D. Case 4: Performance Validation in A Five-Busbar MG

A five-busbar S/T-MG depicted in Fig. 5 is tested in this case. Before the time $t = 4.5$ s, the conventional VSG method and the distributed power sharing method (activated at $t = 1.5$ s) are used in the simulation while the proposed P-VSG method and distributed secondary control method are utilized after $t = 4.5$ s. The simulation results are shown in Fig. 14. From the results, it can be observed that, when the conventional approach is implemented, accurate active and reactive power sharing is asymptotically achieved among DGs based on their ratings. The output active and reactive power of TDGs (about 8.58 kW, 7.01 kVar) is almost twice that of SDGs (about 4.28 kW, 3.46 kVar). However, the voltage magnitude at some buses is beyond the accepted range. Some voltages are higher than the upper limit (320 V) while some are below the lower limit (300 V). Additionally, the VUF at B1 and B2 (about 2.56%) fails to fulfill the requirement of the IEEE 1547 standard. These problems are solved by utilizing the proposed approach after $t = 4.5$ s. It can be observed that, although the active and reactive power cannot accurately be shared among DGs like that of using conventional approach, each phase of the generation units (TDGs and SDGs) can properly share the load power on this phase based on the phase ratings, and the voltages and VUF are also regulated to fulfill the power quality requirements. Compared to the conventional approach, the neutral current of TDG1 (TDG2 is not presented due to page limits.) and the VUF are obviously reduced. VUF at B1 and B2 is reduced by about 31.5% (from 2.56% to 1.75%). At the same time, the accurate phase shift of 120° of the output voltage of the three-phase converters is achieved with the proposed P-VSG method, which is even better than that of the conventional method. The maximum

1949-3053 (c) 2021 IEEE. Personal use is permitted, but republication/redistribution requires IEEE permission. See http://www.ieee.org/publications_standards/publications/rights/index.html for more information.
Authorized licensed use limited to: Aalborg Universitetsbibliotek. Downloaded on February 15,2021 at 09:00:05 UTC from IEEE Xplore. Restrictions apply.

This article has been accepted for publication in a future issue of this journal, but has not been fully edited. Content may change prior to final publication. Citation information: DOI 10.1109/TSG.2021.3057899, IEEE Transactions on Smart Grid

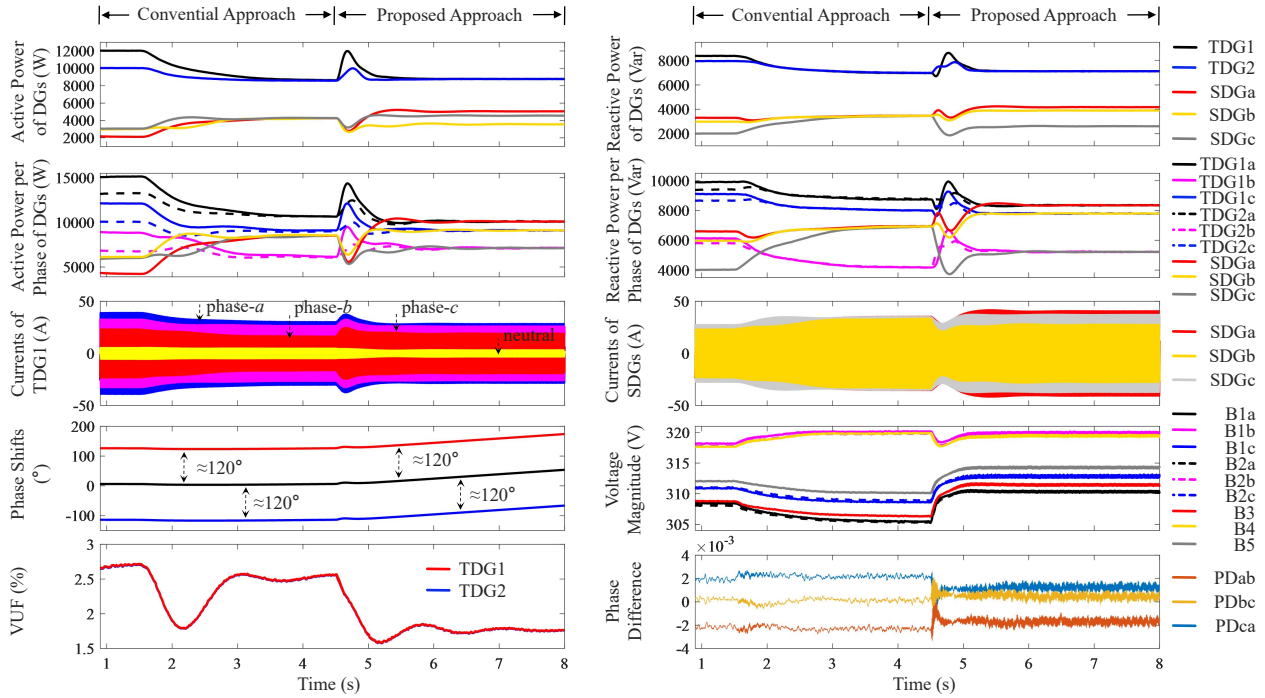

Fig. 14. System performance under case 4 where a five-busbar microgrid is considered.

phase difference at steady state is about 0.00142 (0.17°), which is reduced by approximately 34.6% compared to that of using conventional VSG method (about 0.00215 (0.26°)). This validates the effectiveness of the proposed approach.

Finally, we consider the performance of the proposed control system under the scenario that ESS is full charged and not available. We assume that the total load is less than the source power. Specifically, the ESS in SDGa cannot continue to discharge and is disconnected to prevent damage at $t = 4$ s since the SoC has reached to its minimum value. At $t = 5.5$ s, the ESS in TDG1 is full charged and cannot absorb the energy anymore. The simulation results are shown in Fig. 15, from which it can be observed that the output active power of SDGa is decreased since its ESS is not available. This power deficiency is supplied by TDG1 and TDG2. Consequently, the output power of TDG1 and TDG2 is increased. After $t = 5.5$ s, TDG1 outputs more active power since its ESS has been full charged and the wind power is larger than the output power before $t = 5.5$ s. But the most important thing is that although the output powers of DGs have changed due to the charge and discharge events, the output power can still be kept within the permitted ranges with the proposed approach. We just present the active power results and other results omitted due to the limited space.

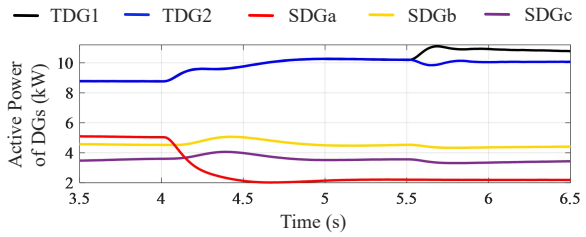

Fig. 15. System performance under case 4 where ESS charge and discharge event is considered.

VI. Conclusion

This paper investigates the power sharing and power quality improvement issues of islanded S/T-MGs with both unbalanced sources and loads and as well as the hybrid RESs/ESSs sources. The proposed control approach includes 1) a P-VSG control used for primary control of DGs, 2) four distributed secondary containment controllers with communication delays used for power sharing among DGs and among phases, voltage restoration and power quality improvement. The proposed P-VSG control allows for independent and flexible power and voltage control for each phase and accurate phase shifts. The distributed secondary controllers based on containment control and constraint operator guarantee admissible output phase powers, voltage profiles, VUF, and permitted values of charging/discharging power of the ESSs, resulting in better operation security and reliability. Simulation results verify the proposed approach and show that unbalance of three-phase power of TDGs is obviously improved and that each phase power is more stable and resilient to load changes.

However, in a real microgrid, different inverters may be manufactured by different manufacturers and these inverters could have different topologies. Therefore, their control methods and operation modes may be different. Some of them may be VSG controlled, some of them may be droop controlled, some of them may be P-VSG controlled, and others may be MPPT controlled. Some DGs may be grid-forming and some others may be grid-following. On the other hand, ESSs are considered and placed at the same power

1949-3053 (c) 2021 IEEE. Personal use is permitted, but republication/redistribution requires IEEE permission. See http://www.ieee.org/publications_standards/publications/rights/index.html for more information.
Authorized licensed use limited to: Aalborg Universitetsbibliotek. Downloaded on February 15,2021 at 09:00:05 UTC from IEEE Xplore. Restrictions apply.

This article has been accepted for publication in a future issue of this journal, but has not been fully edited. Content may change prior to final publication. Citation information: DOI 10.1109/TSG.2021.3057899, IEEE Transactions on Smart Grid

electronics converter in this work. However, ESS may be not available in some areas and some DG units could not have ESS in reality. Information of these DG units could be used to optimize and generate proper leader information for the control system to control the DG units that have available ESS to regulate their outputs to realize the control goal. Moreover, some DGs, like PV and wind power generation units, are not dispatchable. They usually operate in MPPT mode. These factors could affect the performance and practical implementation of the proposed approach. In the future research, we will be committed to studying the issues mentioned above and the practical applications of the proposed approach in actual controllers, and providing hardware implementation and experimental results using the microgrid test system that is being built now to further investigate the performance of this approach and guarantee the implementation feasibility.

APPENDIX

A. Proof of Theorem 1

Proof: Consider the Lyapunov function

$$V(k) = \max_{i,m<\tau_{max}} \{\|x_i(k-m) - \mathcal{P}_Y(x_i(k-m))\|\} \quad (41)$$

From (40) and use similar analysis method in [32], we have

$$\|x_i(k+1) - \mathcal{P}_Y(x_i(k+1))\| \le (1-b_iT)V(k), \quad (42)$$

where $0 < (1-b_iT) = \beta_i(1-p_iT) < 1$. Thus, $V(k+1) \le V(k)$, which means that $V(k)$ is nonincreasing with respect time k. Recall that $V(k) \ge 0$, hence, the limit of $V(k)$ exists.

Suppose that at time kT, there exist two set sequences $\{\mathcal{F}_{P(z)}|z = k, k+1, k+2, \cdots\}$ and $\{\mathcal{F}_{D(z)}|z = k, k+1, k+2, \cdots\}$ such that for all $z \ge k$, $\mathcal{F}_{P(z)} \cup \mathcal{F}_{D(z)} = \mathcal{F}$, $\mathcal{F}_{P(z)} \cap \mathcal{F}_{D(z)} = \emptyset$, $\|x_p(z) - P_Y(x_p(z))\| = V(k)$ holds for follower $p \in \mathcal{F}_{P(z)}$, and $\|x_d(z) - P_Y(x_d(z))\| \le (1-\delta)V(k)$ holds for follower $d \in \mathcal{F}_{D(z)}$ where $0 < \delta < 1$ is a constant. By using similar analysis, we have that $\|x_i(k+C) - P_Y(x_i(k+C))\| < V(k)$ holds for all $C \in \mathfrak{Z}_+$ which means that the agent number in $\mathcal{F}_{P(k+1)}$ is no more than that in $\mathcal{F}_{P(k)}$. Further, the agent number in $\mathcal{F}_{P(k+q)}$ will be zero.

Based on the assumption that there must exist some followers $i_b \in \mathcal{F}$ such that $b_{ib} \ge \mu > 0$, $\|x_{i_b}(k+1) - P_Y(x_{i_b}(k+1))\| \le (1-\mu T)V(k)$. If a follower $i \in \mathcal{F}$ can receive information from a follower j_{b_1} at time $(k+1)T$, we have $\|x_i(k+2+\tau_{ij_{b1}}) - P_Y(x_i(k+2+\tau_{ij_{b1}}))\| \le \left(1-(\mu T)^2\right)V(k)$. By iterations, we further have $\left\|x_{j_{b_1}}(k+2+\tau_{ij_{b1}}) - P_Y(x_{j_{b_1}}(k+2+\tau_{ij_{b1}}))\right\| \le (1-\delta_1)V(k)$. Clearly, all other followers will receive the information from j_{b_1} directly or indirectly in finite time. Since there are at most n following DGs, we can conclude that there exists a finite positive integer $N > q$ such that $\max_{i\in\mathcal{F}} \|x_i(k+N) - P_Y(x_i(k+N))\| \le (1-\delta_N)V(k)$ where $0 < \delta_N < 1$ is a constant. By similar analysis, there exists $0 < \delta_{\overline{N}} < 1$ such that $V(k+N+\tau_{max}) \le (1-\delta_{\overline{N}})V(k)$. It follows that $\lim_{k\to+\infty} V(k) = 0$ and hence, $\lim_{k\to+\infty} \|x_i(k) - P_Y(x_i(k))\| = 0$. Therefore, proper power sharing among DGs, admissible voltage regulation, VUF and ESSs constraints can be realized. The proof is completed. ■

B. Matrix Parameters in (25) and (26)

$$\overline{A}_i = \begin{bmatrix} \tau_i^{-1} & P_{\max,i,\flat} & 0 & 0 & 0 \\ 0 & 0 & 1 & 0 & 0 \\ \frac{-1}{M_i} & 0 & \frac{-D_{p,i}}{M_i} & 0 & 0 \\ 0 & 0 & 0 & -\tau_i^{-1} & -\frac{Q_{\max,i,\flat}}{\tau_i} \\ 0 & 0 & 0 & -K_i^{-1} & -D_{q,i}K_i^{-1} \end{bmatrix},$$

$$\overline{B}_i = \begin{bmatrix} 0 & 0 & 0 & 0 \\ 0 & 0 & 0 & 0 \\ M_i^{-1} & 0 & 0 & 0 \\ 0 & 0 & 0 & 0 \\ 0 & K_i^{-1} & D_{q,i}K_i^{-1} & D_{q,i}K_i^{-1} \end{bmatrix},$$

$$\overline{D}_i = \begin{bmatrix} -\frac{P_{\max,i,\flat}}{\tau_i} & 0 & 0 & 0 & 0 & 0 \\ 0 & 1 & 0 & 0 & 0 & 0 \\ 0 & 0 & M_i^{-1} & 0 & 0 & 0 \\ 0 & 0 & 0 & -\frac{Q_{\max,i,\flat}}{\tau_i} & 0 & 0 \\ 0 & 0 & 0 & 0 & K_i^{-1} & \frac{D_{q,i}}{K_i} \end{bmatrix},$$

$$A_i = \begin{bmatrix} e^{\overline{A}_iT} & 0 \\ 0 & 1-\gamma_i \end{bmatrix}, B_i = \begin{bmatrix} \int_0^T e^{\overline{A}_it}dt\overline{B}_i \\ \widetilde{B}_i \end{bmatrix},$$

$$C_i = \begin{bmatrix} k_{\mathrm{p},i,\flat} & 0 & 0 & 0 & 0 & 0 \\ 0 & 0 & 0 & k_{\mathrm{q},i,\flat} & 0 & 0 \\ 0 & 0 & 0 & 0 & 1 & 0 \\ 0 & 0 & 0 & 0 & 0 & 0 \end{bmatrix}, G = e^{\overline{A}_iT},$$

$$D_i = \begin{bmatrix} \int_0^T e^{\overline{A}_it}dt\overline{D}_i & 0 \\ 0 & \frac{\eta_{\mathrm{ess},i}}{E_{\mathrm{ess},i}}T \end{bmatrix}, \sigma_i = \left(\sum_{j\in\mathcal{N}_i} a_{ij} + c\right),$$

$\widetilde{B}_i = \begin{bmatrix} \frac{\eta_{\mathrm{ess},i}T}{E_{\mathrm{ess},i}} & 0 & 0 & 0 \end{bmatrix}$, $H = \int_0^T e^{\overline{A}_it}dt\overline{B}_i$, $F = \int_0^T e^{\overline{A}_it}dt\overline{D}_i$.

C. Matrix Parameters in (40)

$$\mathbf{A}_i = \begin{bmatrix} A & B \\ \beta_i\sigma_iC_i & (1-b_iT)I \end{bmatrix}, \mathbf{A}_j = \begin{bmatrix} O & O \\ \beta_iC_j & O \end{bmatrix},$$
$$\mathbf{B}_i = \begin{bmatrix} O \\ \beta_icI \end{bmatrix}, \mathbf{C}_i = \begin{bmatrix} C_i & O \end{bmatrix}, \mathbf{D}_i = \begin{bmatrix} D \\ O \end{bmatrix}.$$

REFERENCES

[1] J. M. Guerrero, M. Chandorkar, T.-L. Lee, and P. C. Loh, "Advanced control architectures for intelligent microgrids-part I: decentralized and hierarchical control," *IEEE Trans. Ind. Electron.*, vol. 60, no. 4, pp. 1254-1262, Apr. 2013.

[2] R. Han, L. Meng, J. M. Guerrero, and J. C. Vasquez, "Distributed nonlinear control with event-triggered communication to achieve current-sharing and voltage regulation in DC microgrids," *IEEE Trans. Power Electron.*, vol. 33, vol. 7, pp. 6416-6433, Jul. 2018.

[3] H. Zhang, S. Kim, Q. Sun and J. Zhou, "Distributed adaptive virtual impedance control for accurate reactive power sharing based on consensus control in microgrids," *IEEE Trans. Smart Grid*, vol. 8, no. 4, pp. 1749-1761, Jul. 2017.

[4] P. Wang, C. Jin, D. Zhu, Y. Tang, P. C. Loh and F. H. Choo, "Distributed control for autonomous operation of a three-port AC/DC/DS hybrid microgrid," *IEEE Trans. Ind. Electron.*, vol. 62, no. 2, pp. 1279-1290, Feb. 2015.

[5] J. Zhou, S. Kim, H. Zhang, Q. Sun and R. Han, "Consensus-based distributed control for accurate reactive, harmonic and imbalance power sharing in microgrids," *IEEE Trans. Smart Grid*, vol. 9, no. 4, pp. 2453-2467, Jul. 2018.

[6] J. He, Y. W. Li, and F. Blaabjerg, "Flexible microgrid power quality enhancement using adaptive hybrid voltage and current controller," *IEEE Trans. Ind. Electron.*, vol. 61, no. 6, pp. 2784-2794, Jun. 2014.

1949-3053 (c) 2021 IEEE. Personal use is permitted, but republication/redistribution requires IEEE permission. See http://www.ieee.org/publications_standards/publications/rights/index.html for more information.
Authorized licensed use limited to: Aalborg Universitetsbibliotek. Downloaded on February 15,2021 at 09:00:05 UTC from IEEE Xplore. Restrictions apply.

This article has been accepted for publication in a future issue of this journal, but has not been fully edited. Content may change prior to final publication. Citation information: DOI 10.1109/TSG.2021.3057899, IEEE Transactions on Smart Grid

[7] A. Hintz, U. R. Prasanna and K. Rajashekara, "Comparative study of the three-phase grid-connected inverter sharing unbalanced three-phase and/or single-phase systems," *IEEE Trans. Ind. Appl.*, vol. 52, no. 6, pp. 5156-5164, Nov.-Dec. 2016.

[8] L. Wang, R. Yan, F. Bai, T. Saha and K. Wang, "A distributed inter-phase coordination algorithm for voltage control with unbalanced PV integration in LV systems," *IEEE Trans. Sustain. Energy*, vol. 11, no. 4, pp. 2687-2697, Oct. 2020.

[9] D. Schwanz, F. Möller, S. K. Rönnberg, J. Meyer and M. H. J. Bollen, "Stochastic Assessment of Voltage Unbalance Due to Single-Phase-Connected Solar Power," *IEEE Trans. Power Delivery*, vol. 32, no. 2, pp. 852-861, Apr. 2017.

[10] J. He, Y. Wei-Li and F. Blaabjerg, "An enhanced islanding microgrid reactive power, imbalance power, and harmonic power sharing scheme," *IEEE Trans. Power Electron.*, vol. 30, no. 6, pp. 3389-3401, 2015.

[11] E. Espina, R. Cárdenas-Dobson, M. Espinoza-B., C. Burgos-Mellado and D. Sáez, "Cooperative regulation of imbalances in three-phase four-wire microgrids using single-phase droop control and secondary control algorithms," *IEEE Trans. Power Electron.*, vol. 35, no. 2, pp. 1978-1992, Feb. 2020.

[12] B. Liu, Z. Liu, J. Liu, R. An, H. Zheng and Y. Shi, "An adaptive virtual impedance control scheme based on small-ac-signal injection for unbalanced and harmonic power sharing in islanded microgrids," *IEEE Trans. Power Electron.*, vol. 34, no. 12, pp. 12333-12355, Dec. 2019.

[13] Q. Sun, J. Zhou, J. M. Guerrero, and H. Zhang, "Hybrid three-phase/singlephase microgrid architecture with power management capabilities, *IEEE Trans. Power Electron.*, vol. 30, no. 10, pp. 5964-5977, Oct. 2015.

[14] S. A. Raza and J. Jiang, "Intra- and inter-phase power management and control of a residential microgrid at the distribution level," *IEEE Trans. Smart Grid*, vol. 10, no. 6, pp. 6839-6848, Nov. 2019.

[15] Y. Karimi, H. Oraee and J. M. Guerrero, "Decentralized method for load sharing and power management in a hybrid single/three-phase-islanded microgrid consisting of hybrid source PV/battery units," *IEEE Trans. Power Electron.*, vol. 32, no. 8, pp. 6135-6144, Aug. 2017.

[16] M. A. Allam, A. A. Said, M. Kazerani and E. F. El Saadany, "A novel dynamic power routing scheme to maximize loadability of islanded hybrid AC/DC microgrids under unbalanced AC loading," *IEEE Trans. Smart Grid*, vol. 9, no. 6, pp. 5798-5809, Nov. 2018.

[17] J. Zhou, Y. Xu, H. Sun, Y. Li, and M.-Y. Chow, "Distributed power management for networked AC/DC microgrids with unbalanced microgrids," *IEEE Trans. Ind. Inform.*, vol. 16, no. 3, pp. 1655-1667, Mar. 2020.

[18] L. Meng and J. M. Guerrero, "Optimization for customized power quality service in multibus microgrids," *IEEE Trans. Ind. Electron.*, vol. 64, no. 11, pp. 8767-8777, Nov. 2017.

[19] M. M. Hashempour, T. Lee, M. Savaghebi and J. M. Guerrero, "Real-time supervisory control for power quality improvement of multi-area microgrids," *IEEE Syst. J.*, vol. 13, no. 1, pp. 864-874, Mar. 2019.

[20] Y. Li, W. Gao, and W. Yan et al., "Data-Driven Optimal Control Strategy for Virtual Synchronous Generator via Deep Reinforcement Learning Approach," *Journal of Modern Power Systems and Clean Energy*, to be pulished, doi: 10.35833/MPCE.2020.000267..

[21] L. Meng, X. Zhao, F. Tang, M. Savaghebi, T. Dragicevic, J. C. Vasquez and J. M. Guerrero, "Distributed voltage unbalance compensation in islanded microgrids by using a dynamic consensus algorithm," *IEEE Trans. Power Electron.*, vol. 31, no. 1, pp. 827-838, Jan. 2016.

[22] S. Yan, M. Wang, T. Yang, S. Tan, B. Chaudhuri and S. Y. R. Hui, "Achieving multiple functions of three-phase electric springs in unbalanced three-phase power systems using the instantaneous power theory," *IEEE Trans. Power Electron.*, vol. 33, no. 7, pp. 5784-5795, Jul. 2018.

[23] D. I. Brandao, T. Caldognetto, F. P. Marafão, M. G. Simões, J. A. Pomilio and P. Tenti, "Centralized control of distributed single-phase inverters arbitrarily connected to three-phase four-wire microgrids," *IEEE Trans. Smart Grid*, vol. 8, no. 1, pp. 437-446, Jan. 2017.

[24] F. Nejabatkhah and Y. W. Li, "Flexible unbalanced compensation of three-phase distribution system using single-phase distributed generation inverters," *IEEE Trans. Smart Grid*, vol. 10, no. 2, pp. 1845-1857, Mar. 2019.

[25] A. Mortezaei, M. G. Simões, M. Savaghebi, J. M. Guerrero, and A. Al-Durra, "Cooperative control of multi-master-slave islanded microgrid with power quality enhancement based on conservative power theory," *IEEE Trans. Smart Grid*, vol. 9, no. 4, pp. 2964-2975, Jul. 2018.

[26] D. I. Brandao, L. S. Araujo, A. M. S. Alonso, G. L. dos Reis, E. V. Liberado and F. P. Marafão, "Coordinated control of distributed three- and single-phase inverters connected to three-phase three-wire microgrids," *IEEE J. Emerg. Sel. Topics Power Electron.*, to be published, doi:10.1109/JESTPE.2019.2931122.

[27] IEEE standard for interconnection and interoperability of distributed energy resources with associated electric power systems interfaces, IEEE Std 1547TM-2018, Feb. 2018.

[28] C. Burgos-Mellado, R. Cárdenas, D. Sáez, A. Costabeber and M. Sumner, "A control algorithm based on the conservative power theory for cooperative sharing of imbalances in four-wire systems," *IEEE Trans. Power Electron.*, vol. 34, no. 6, pp. 5325-5339, Jun. 2019.

[29] C. Burgos-Mellado, J. J. Llanos, R. Cárdenas, D. Sáez, D. E. Olivares, M. Sumner and A. Costabeber, "Distributed control strategy based on a consensus algorithm and on the conservative power theory for imbalance and harmonic sharing in 4-wire microgrids," *IEEE Trans. Smart Grid*, vol. 11, no. 2, pp. 1604-1619, Mar. 2020.

[30] Q. Zhong, "Virtual synchronous machines: A unified interface for grid integration," *IEEE Power Electron. Mag.*, vol. 3, no. 4, pp. 18-27, Dec. 2016.

[31] J. Liu, Y. Miura, H. Bevrani and T. Ise, "Enhanced virtual synchronous generator control for parallel inverters in microgrids," *IEEE Trans. Smart Grid*, vol. 8, no. 5, pp. 2268-2277, Sept. 2017.

[32] P. Lin, W. Ren, and H. Gao, "Distributed velocity-constrained consensus of discrete-time multi-agent systems with nonconvex constraints, switching topologies, and delays," *IEEE Trans. Autom. Control*, vol. 62, no. 11, pp. 5788-5794, Nov. 2017.

[33] J. S. Giraldo, J. A. Castrillon, J. C. López, M. J. Rider and C. A. Castro, "Microgrids energy management using robust convex programming," *IEEE Trans. Smart Grid*, vol. 10, no. 4, pp. 4520-4530, Jul. 2019.

[34] S. Golestan, J. M. Guerrero, J. C. Vasquez, A. M. Abusorrah and Y. Al-Turki, "All-pass-filter-based PLL systems: linear modeling, analysis, and comparative evaluation," *IEEE Trans. Power Electron.*, vol. 35, no. 4, pp. 3558-3572, Apr. 2020.

[35] S. Golestan, J. M. Guerrero, J. C. Vasquez, A. M. Abusorrah and Y. Al-Turki, "Modeling, tuning, and performance comparison of second-order-generalized-integrator-based FLLs," *IEEE Trans. Power Electron.*, vol. 33, no. 12, pp. 10229-10239, Dec. 2018.

[36] Q. Zhong, G. C. Konstantopoulos, B. Ren and M. Krstic, "Improved synchronverters with bounded frequency and voltage for smart grid integration," *IEEE Trans. Smart Grid*, vol. 9, no. 2, pp. 786-796, Mar. 2018.

[37] Q. Zhong, P. Nguyen, Z. Ma and W. Sheng, "Self-synchronized synchronverters: inverters without a dedicated synchronization unit," *IEEE Trans. Power Electron.*, vol. 29, no. 2, pp. 617-630, Feb. 2014.

[38] R. Aouini, B. Marinescu, K. Ben Kilani and M. Elleuch, "Synchronverter-based emulation and control of HVDC transmission," *IEEE Trans. Power Syst.*, vol. 31, no. 1, pp. 278-286, Jan. 2016.

[39] IEEE Standard for Exchanging Information Between Networks Implementing IEC 61850 and IEEE Std 1815(TM) [Distributed Network Protocol (DNP3)], *IEEE Std 1815.1-2015.* (Incorporates IEEE Std 1815.1-2015/Cor 1-2016)

[40] B. K. Poolla, D. Groß and F. Dörfler, "Placement and implementation of grid-forming and grid-following virtual inertia and fast frequency response," *IEEE Trans. Power Syst.*, vol. 34, no. 4, pp. 3035-3046, Jul. 2019.

[41] D. Pattabiraman, R. H. Lasseter. and T. M. Jahns, "Comparison of grid following and grid forming control for a high inverter penetration power system," *in Proc. IEEE Power Energy Society General Meeting (PESGM)*, Portland, OR, USA, Aug. 2018, pp. 1-5.

Jianguo Zhou (M'19) received the B.S. degree in Automation and the M.S. and Ph.D. degrees in Control Theory and Control Engineering from Northeastern University, Shenyang, China, in 2011, 2013 and 2018, respectively.

Since December 2018, he has been a postdoctoral researcher with the Tsinghua-Berkeley Shenzhen Institute (TBSI), Tsinghua Shenzhen International Graduate School (TsinghuaSIGS), Tsinghua University, Shenzhen, China. His current research interests include power electronics, distributed control and optimization with applications in microgrids, virtual power plant and Energy Internet.

1949-3053 (c) 2021 IEEE. Personal use is permitted, but republication/redistribution requires IEEE permission. See http://www.ieee.org/publications_standards/publications/rights/index.html for more information.
Authorized licensed use limited to: Aalborg Universitetsbibliotek. Downloaded on February 15,2021 at 09:00:05 UTC from IEEE Xplore. Restrictions apply.

This article has been accepted for publication in a future issue of this journal, but has not been fully edited. Content may change prior to final publication. Citation information: DOI 10.1109/TSG.2021.3057899, IEEE Transactions on Smart Grid

Hongbin Sun (SM'12-F'17) received his double B.S. degrees from Tsinghua University in 1992, the Ph.D from Dept. of E.E., Tsinghua University in 1996. From 2007.9 to 2008.9, he was a visiting professor with School of EECS at the Washington State University in Pullman.

He is now ChangJiang Scholar Chair professor in Dept. of E.E. and the director of energy management and control research center, Tsinghua University. He is currently IEEE Fellow and IET Fellow. He also serves as the editor of the IEEE TSG, associate editor of IET RPG, and member of the Editorial Board of four international journals and several Chinese journals. His technical areas include electric power system operation and control with specific interests on the Energy Management System, System-wide Automatic Voltage Control, and Energy System Integration. He has published more than 400 peer-reviewed papers, within which over 60 are IEEE and IET journal papers, and 4 books. He has been authorized 5 US Patents of Invention and more than 100 Chinese Patents of Invention.

Yinliang Xu (M'13-SM'19) received the B.S. and M.S. degrees in Control Science and Engineering from Harbin Institute of Technology, China, in 2007 and 2009, respectively, and the Ph.D. degree in Electrical and Computer Engineering from New Mexico State University, Las Cruces, NM, USA, in 2013.

He is now an Assistant Professor with TsinghuaBerkeley Shenzhen Institute (TBSI), Lab of Smart Grid and Renewable Energy, Shenzhen, Guangdong, China. From Sept. 2015 to Aug. 2018, he was an adjunct faculty with Department of Electrical and Computer Engineering at Carnegie Mellon University, Pittsburgh, PA, USA. From Nov. 2013 to Aug. 2017, he was with School of Electronics and Information Technology, Sun Yat-Sen University. From 2013 to 2014, he was a Visiting Scholar with the Department of Electrical and Computer Engineering, Carnegie Mellon University, Pittsburgh, PA, USA His research interests include distributed control and optimization of power systems, renewable energy integration and microgrid modeling and control.

Renke Han (S'16-M'18) received the B.S. degree in Automation, the M.S. degree in Control Theory and Control Engineering both from Northeastern University, Liaoning, China, in 2013 and 2015 respectively. He received the Ph.D. degree in Power Electronics Systems from Aalborg University, Aalborg, Denmark, in 2018.

From February 2017 to September 2017, he was as a Visiting Scholar with Laboratoire d'Automatique, École Polytechnique Fédérale de Lausanne (EPFL), Lausanne, Switzerland. Since November 2018, he has been with Power Electronics Group, University of Oxford, UK, as a postdoctoral researcher. His research interests include power electronics converter design including PCB design for power and control circuitries and magnetic elements design, embedded system development, modeling, control and stability analysis for Microgrid.

He was selected as one of six research representatives by University of Oxford, attending Global Young Scientist Summit (GYSS) 2021. He received an outstanding presentation award in Annual Conference of the IEEE Industrial Electronics Society, Italy in 2016 and the Outstanding Master Degree Thesis Award from Liaoning Province, China, in 2014.

Zhongkai Yi (S'16) received the B.S. and M.S. degrees in Electrical Engineering from Harbin Institute of Technology, China, in 2016 and 2018, respectively. He is currently pursuing the Ph.D. degree with Tsinghua-Berkeley Shenzhen Institute (TBSI), Tsinghua Shenzhen International Graduate School (Tsinghua SIGS), Tsinghua University.

His current research interests include optimization and control of integrated energy system, modeling and operation of virtual power plant.

Liming Wang (M'10-SM'18) was born in Zhejiang province, China, on 30 November 1963. He received the B.S., M.S., and Ph.D. degrees in high voltage engineering from the Department of Electrical Engineering, Tsinghua University, Beijing, P.R. China, in 1987, 1990, and 1993, respectively.

He started to work at Tsinghua University in 1993 and has been a full professor since 2002. He is now the director of Institute of Energy and Advanced Electrical Technology, Graduate School at Shenzhen, Tsinghua University. His major research fields include high voltage insulation and electrical discharge, flashover mechanism on contaminated insulators, and application of pulsed electric fields. He is the Chair of IEEE Dielectrics and Electrical Insulation Society Technical committee Discharges in Air at UHV, member of CIGRE SC D1, member of CIGRE B2 69. He has published over 300 peer-reviewed papers, more than 65 of which are IEEE Transaction papers.

Josep M. Guerrero (S'01-M'04-SM'08-FM'15) received the B.S. degree in telecommunications engineering, the M.S. degree in electronics engineering, and the Ph.D. degree in power electronics from the Technical University of Catalonia, Barcelona, in 1997, 2000 and 2003, respectively. Since 2011, he has been a Full Professor with the Department of Energy Technology, Aalborg University, Denmark, where he is responsible for the Microgrid Research Program. From 2014 he is chair Professor in Shandong University; from 2015 he is a distinguished guest Professor in Hunan University; and from 2016 he is a visiting professor fellow at Aston University, UK, and a guest Professor at the Nanjing University of Posts and Telecommunications. From 2019, he became a Villum Investigator by The Villum Fonden, which supports the Center for Research on Microgrids (CROM) at Aalborg University, being Prof. Guerrero the founder and Director of the same centre (www.crom.et.aau.dk).

His research interests is oriented to different microgrid aspects, including power electronics, distributed energy-storage systems, hierarchical and cooperative control, energy management systems, smart metering and the internet of things for AC/DC microgrid clusters and islanded minigrids. Specially focused on microgrid technologies applied to offshore wind, maritime microgrids for electrical ships, vessels, ferries and seaports, and space microgrids applied to nanosatellites and spacecrafts. Prof. Guerrero is an Associate Editor for a number of IEEE TRANSACTIONS. He has published more than 600 journal papers in the fields of microgrids and renewable energy systems, which are cited more than 60,000 times. He received the best paper award of the IEEE Transactions on Energy Conversion for the period 2014-2015, and the best paper prize of IEEE-PES in 2015. As well, he received the best paper award of the Journal of Power Electronics in 2016. During seven consecutive years, from 2014 to 2020, he was awarded by Clarivate Analytics (former Thomson Reuters) as Highly Cited Researcher with 50 highly cited papers. In 2015 he was elevated as IEEE Fellow for his contributions on distributed power systems and microgrids.

1949-3053 (c) 2021 IEEE. Personal use is permitted, but republication/redistribution requires IEEE permission. See http://www.ieee.org/publications_standards/publications/rights/index.html for more information.
Authorized licensed use limited to: Aalborg Universitetsbibliotek. Downloaded on February 15,2021 at 09:00:05 UTC from IEEE Xplore. Restrictions apply.